Vertical Axis Wind Turbine for Remote Power Generation

Worcester MA, 01609

A Major Qualifying Project
Submitted to the Faculty of
WORCESTER POLYTECHNIC INSTITUTE
in Partial Fulfillment of the Requirements for the
Degree of Bachelor Science

Student Authors
Jeremy Lane
Theodore Lynn
Saffiyah Rafieck
Travis M. Rossen

Project Advisors
Professor Brian J Savilonis

April 25, 2018

Abstract

The goal of this project was to create a working microturbine capable of charging small electronic devices, constructed using materials readily available in off-grid locations, such as developing countries or areas recently affected by natural disasters. Given the target audience, the design was focused on minimizing the amount of machining by modifying off-the-shelf products to create turbine components. A full-scale prototype was constructed and field-tested to determine its performance characteristics under an electric load at various wind speeds. Testing showed that with a resistive load of 20 ohms the turbine has a maximum system efficiency of 13 percent and produced a maximum power of 4 Watts in 6 m/s of wind. Based upon the prototype's performance, with the proper charging circuit the turbine could be adapted to charge small electronic devices such as battery packs or cell phones.

Table of Contents

Table of Figures

Table of Tables

1. Introduction

Not only is energy usage a concern for big cities where millions of people expect their power to come on, but it is also a problem for the number of people who live off "the grid" and do not have access to electricity from a power plant. They are often forced to use fuel-burning generators and other means to create the power they use or they must deal with the reality of not having electricity in their lives. While some people choose to go off grid in order to meet their own needs without relying upon the outside world, others are forced into this living situation. In both cases those who depend upon generators for power must rely on supply runs for their fuel which limits their ability to be self-sufficient.

The growing number and severity of natural disasters, such as hurricanes and tornadoes has led to an increase in destruction of developed areas leaving hundreds of thousands of people without electricity for extended periods of time. Given the severity of some storms, response time for the resources necessary for reconstruction is slow, making it difficult to rebuild vital infrastructure such as electric grids in a timely fashion. For example, in 2017 Hurricane Maria destroyed the entire electrical grid in Puerto Rico, leaving the entire island without power. Even three months after the hurricane hit nearly half the population in Puerto Rico was still without power; and it was predicted that some areas would not get power until at least 8 months after the storm[1], [2]. More than two months after Hurricanes Irma and Maria hit the U.S. Virgin Islands, over 73% of customers were still without power[3].

While many people in such devastated areas use generators, not everyone can afford or obtain a generator or the fuel to operate it for 2, 3, or 8 months, and sufficient fuel might not be readily available. However, the destruction usually results in a vast quantity of resources

available to be repurposed to produce a temporary power source such as a small wind turbine. For example, in St. Thomas alone, Hurricane Irma produced over 736,000 cubic yards of debris[4]. Much of that debris contains items such as metal poles, lengths of PVC pipe, plywood, plastic sheeting and, in coastal areas, sails, masts, and rigging that might no longer be useful for its original purpose or for large-scale projects, but could be repurposed to create small wind turbines to generate energy, enabling people to generate enough electricity for essential tasks during the weeks or months that the power grid is being repaired.

The goal of this project was to create an easy-to-construct, cheap, and effective small-scale wind turbine that could provide a possible temporary solution to energy shortages by repurposing materials readily available in off-grid locations, such as developing countries or areas recently affected by natural disasters. Given the understanding that the people interested in this turbine would be in disaster relief areas or in off-grid locations, there were a number of constraints that this project had to address. First, the turbine must produce a minimum of 2.5 Watts of electrical power in order to charge a cellphone battery. Second, the turbine must have a cut-in speed of 4 m/s so that it will produce power under normal wind conditions. Third given our target audience, the turbine must be designed so most of the parts could be salvaged after a disaster or would be readily available at a hardware store. Finally, to ensure our target audience would be able to complete the build, the project must use minimal tooling to ensure that a normal person with moderate technical skills can complete it.

2. Background

2.1 Renewable energy

By definition a renewable energy is “any naturally occurring, theoretically inexhaustible source of energy, [such] as biomass, solar, wind, tidal, wave, and hydroelectric power, which is not derived from fossil or nuclear fuel[5].” By this definition, we see that this is an energy source that is inexhaustible, which means while we may run out of things such as oil, natural gas, and coal, we will never run out of sunlight, wind, or moving water. These methods of power production cause little negative effects on the ecosystem, and as long as they are maintained, can continue to produce clean energy. While renewable energy was made popular in the 1960’s and 70’s with the Environmental Movement, some of the main technologies have been around for thousands of years in the form of mechanical energy[6].

One of the major sources of renewable energy is wind power. This method uses the rotation of blades to transform the energy from the wind into mechanical power. Historically, wind turbines have been used to both pump water from the ground and to grind down grain. Today, generators are coupled with wind turbines to create electricity for the power grid[7]. Wind energy generates 228,480,000 MWh of power or 5.6% of the energy produced in the United States every year, making it the second largest source of renewable energy behind hydropower[8].

Most methods of renewable energy are often thought of only on the large scale with megawatts of power being created; however, this is not always the case. For example, in 2017 there was a significant number of people who either already had personal renewable energy systems at their homes or wished to have these systems installed[9]. These small-scale systems

have been on the rise as both governments and individuals have noticed the importance of protecting the environment for the future. Small-scale renewable energy also provides people who wish to be off-grid the ability to be more self-reliant and produce their own energy, as well as the people who simply do not have access to reliable energy, for example in developing countries or places where natural disasters have occurred.

2.2 Power in the wind

Wind turbines generate power by taking the potential energy from the wind and transforming it into kinetic rotational energy. This is done by creating a pressure difference between the air before it enters the turbine and the air that has passed through the turbine[10]. As the air flows through the turbine it is disrupted by the rotating blades and slowed down. Since air can be considered incompressible at low velocities, the air pressure is decreased to below atmospheric conditions just after passing through the turbine[10]. In order to maintain equilibrium the air must eventually return to the surrounding air pressure. Consequently, the resulting increase in pressure occurs at the price of a drop of kinetic energy. Eventually, after the stream flows a substantial distance past the turbine it returns to the pressure and velocity of the surrounding air[10].

Calculating the exact amount of power a turbine can extract from the wind is complex and requires an understanding of fluid dynamics, and airfoil geometry. However, the power curve for a turbine (a plot of the turbine's power at various wind speeds) can be estimated using much simpler calculations based upon the theoretical maximum amount of energy in any given amount of air[11]. This value can be obtained from Equation 1.

$$(1) \qquad Power = \frac{1}{2}\rho A_{swept} v^3$$

Where P equals Power, ρ equals the density of the air at the given atmospheric conditions, A_{swept} is the swept area of the turbine and v is the upstream velocity of the wind. Swept area is total cross sectional area that the blades pass through as they rotate. The swept area of a horizontal axis turbine, for example, is the area of the circle that connects the three blades together[11].

Since the density of the air is both difficult to change and relatively constant for a given area, the main factor that influences power generation is wind speed. Doubling the turbine's swept area will only double the turbine's power output. However, doubling the wind speed will provide a significant increase in the turbine's power output. For example, if a turbine generates 27 W at a wind speed 3 m/s, it could theoretically generate 216 W at 6 m/s.

2.3 Cut-in and cut-out speed

Cut-in speed is the wind velocity at which the turbine will start spinning and producing power. For most horizontal axis turbines, the cut-in speed is typically around wind velocities of 5 m/s, whereas some vertical axis turbines have cut-in speeds as low as 2 m/s[12]. Cut-out speed is the wind velocity at which the turbine will cease to spin, thus no longer producing power. Cut-out speed is not limited by the power in the wind, but rather by the strength of the materials used in the turbine's construction. Higher speed produces more power, but it also spins the blades faster and applies more force on the structure, which at a certain point may cause the structure to become unstable and fail. As a result, the cut-out speed was developed to protect the turbine. For many commercial turbines the cut-out speed is around 25 m/s although there are turbines that can operate safely in much higher wind conditions[10].

2.4 Coefficient of Power

Like all systems, actual turbines do not operate under ideal conditions. The existence of drag, friction and other phenomena limit a turbine's power output. The coefficient of power (C_p) is the fraction or percentage of the total power in the wind that the turbine extracts. Cp can be calculated using Equation 2.

$$(2) \qquad C_p = \frac{Power\ from\ Turbine}{Total\ Power\ from\ Wind} = \frac{Turbine\ Power}{\frac{1}{2}\rho A_{swept} v^3}$$

The maximum theoretical value for the coefficient of power is 0.593 as determined by the Betz limit[10]. However, most commercial horizontal axis turbines have coefficients of power around 40 percent[11].

2.5 Tip Speed Ratio

Calculating the rotational velocity of the turbine's main shaft is important because it determines how much electricity or mechanical power the turbine generates. As seen in Equation 3, Tip Speed Ratio (TSR or λ) is defined as the ratio of the speed of the blade tip to the upstream wind speed, and thus it relates the velocity of the wind to the angular velocity of the rotor[10]-[12].

$$(3) \qquad \lambda = \frac{R\omega}{v}$$

In Equation 3, λ is the TSR, R corresponds to the radius of the turbine, ω is the angular velocity of the turbine blades, and v is the velocity of the wind.

Higher TSRs correspond to more power, but smaller amounts of torque, whereas lower TSRs correspond to higher torques, but lower angular velocities. Horizontal axis turbines, which are typically used to produce electricity, operate with TSRs around six, while Vertical axis turbines, which are used for both mechanical power or electricity production, operate at lower TSRs ranging from less than one to about three, although some designs can have TSR as high as six[10]-[13].

2.6 Airfoil Shapes

Typically turbine blades are constructed out of various airfoil shapes and designs[10]-[13]. Airfoils are an engineered shape used most commonly as the cross sectional shape of an airplane wing[14]. These shapes were chosen for their ability to create a pressure difference across the top and bottom of the wing[15]. As can be seen from Figure 1, a typical airfoil consists of a rounded front called the leading edge, and a pointed tail called the trailing edge[10]. Because of the shape of the airfoil, the air is forced over the top of edge of the airfoil and must move at a higher velocity than the air moving along the bottom edge[15]. This creates a localized high pressure below the wing and an area of lower pressure above the wing. As the airfoil moves, the air is forced to flow around it, which creates an upward force on the wing called lift[15]. This lift force is what allows airplanes to take off[14]. The airfoil properties can be applied to turbines as well. The airfoils that create the geometry of the blades are oriented in such a manner that the lift force translates into rotational movement, which spins the shaft of the generator, and creates electricity. However, due to the different conditions turbine blades experience, the geometry of the airfoil shapes used to create them differs slightly from the

airfoils used in airplanes[13]. Airplane wings are designed to be flexible and operate at high speeds with low angles of attack[14]. Angle of attack is the angle between the chord line and the direction of airflow, which is alpha in Figure 1. Consequently, wings are typically created out of thin airfoils. This means they have a chord to thickness ratio of less than 10%[14]. Wind turbines, however, operate at slower speeds and must remain rigid so as not to crash into the turbine's tower[13]. As a result, turbine blades are typically created out of thicker airfoils

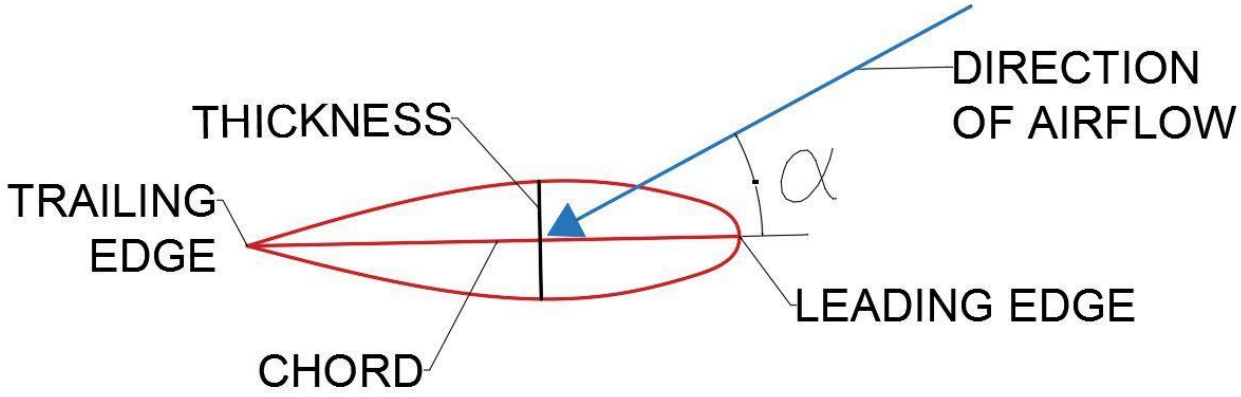

Figure 1: Description of airfoil terminology

(thickness ratios around 16-25%) because they are stiffer, remain more rigid, and are most efficient at lower speeds and higher angles of attack[13].

2.7 Horizontal Axis Turbine

The horizontal axis turbine is a turbine that was initially developed in the first century AD by Heron of Alexandria to power basic machines[7]. Initially these turbines were used to produce mechanical power for grinding grain but now they mainly are used to generate electricity. As can be seen in Figure 2, a HAWT consists of a vertical shaft that runs almost the entire length of the turbine. On top of the shaft is a housing that holds the key components to generating power. First, at the end of the housing is the rotor which focuses on capturing the

maximum amount of wind over the blades of the turbines. These blades are usually set up in a circular pattern and are angled to capture the force of the wind and get the most power out of it. These blades are then attached to a horizontal shaft that runs inside the housing and attaches to a gearbox. The gearbox is a gear setup that increases the rotational speed of a shaft. From there the gear box feeds into the generator which is the heart of the turbine and is what turns raw mechanical power into electricity[16].

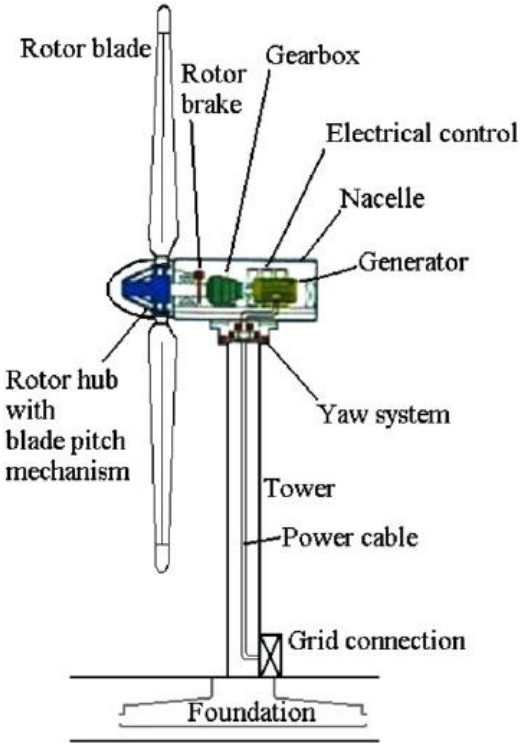

Figure 2: Horizontal axis turbine[16]

This style of turbine is the conventional design most commonly used turbine type. However, it has both pros and cons that go along with it. One benefit of horizontal wind turbines is that they have a strong tower base that allows for stability and good performance in high winds. Another advantage is that they are very functional and efficient due to the blade geometry and they do not require backtracking. Disadvantages to horizontal axis turbines are that they not only have a high initial cost, they also have a high upkeep cost that makes them harder for the

average person to own. They also need to be constructed correctly or in high winds they could destroy themselves[17].

2.8 Darrieus Turbine

The Darrieus is a vertical axis turbine that was developed in France during the 1920's by Georges Jean Marie Darrieus, an aeronautical engineer [18]. The turbine was designed as a biomimicry of bird wings [18]. The turbine consists of a central shaft mounted vertically the air. The blades are connected at the top and the bottom of the shaft and extend outwards in a parabolic shape creating the impression of an egg-beater [12]. Darrieus turbines works on the principle that if the blades spin faster than the wind, the apparent wind seen by the airfoil-shaped blades becomes greater than zero[12], [18]. This creates a lift force that propels the turbine forward continuing the cycle. The optimal range of for the angle of attack is between -20 and 20 degrees. Any angle greater than this creates turbulence along the blade, which lessens the forward-pushing lift force[18]. Unfortunately, because the Darrieus requires the apparent wind to be at an angle greater than zero, it is difficult for them to self-start. However, the Darrieus style turbine does have some features that help make up for this drawback. First, because the blades are symmetrical and vertically mounted, it does not need to be oriented into the wind. This eliminates the need for a costly yaw system. Second, because the blades are attached at both the top and the bottom of the turbine shaft, they only experience tensile loading and do not need to be tapered at the end, like the blades on a horizontal axis turbine[12]. This makes them easier to manufacture and less likely to fail due to fatigue. Third, the egg-beater shape allows the turbine to self-regulate its rotational velocity and remain at the optimal speed regardless of the wind

velocity[12]. This phenomenon is due to the change in lift created along the blade. At the center of the blade, where the radius is widest, the blades produce the maximum amount of lift and forward motion. However, the top and bottom of the blade are not situated at the optimal angle of attack and thus stall out, which slows the turbine down, allowing it to regulate speed.

The original Darrieus turbine blades were created out of symmetrical airfoils similar to the NACA 0015 and 0018 airfoil shapes[18]. The theory was that the symmetrical airfoil would maximize the lift created by the blades since the blades could generate lift from both sides. However, Darrieus turbines did have some flaws. The cyclical switching between positive and negative angles of attack caused the turbines to vibrate violently and generate lots of noise[19]. Additionally, the curvature of the blades limited the percentage of the blade that actually generates usable lift. On large turbines this was not a huge issue as most of the blade operated within the effective angle of attack range; however, on smaller microturbines, this design flaw leads to a relatively inefficient turbine[19]. As a result, various modifications to the Darrieus have been implemented. These include straightening the blades in order to maximize the area operating in the effective angle of attack range, and increasing the number of blades to better balance the turbine and increase its efficiency[19].

2.9 Savonius Turbine

Savonius wind turbines, seen in Figure 3, are drag-driven devices with a vertical axis rotor generally comprised of two oppositely curved surfaces. Each rotor surface typically has a semicircular profile formed by cutting a cylinder in half through its axis. Torque on the rotor is produced due to the drag force on the surface that is concave relative to the wind direction being greater than the drag force on the convex surface[20]. The rotor halves can also be overlapped

slightly at the axis of rotation in order to allow air to flow between each half, resulting in additional positive torque from the aerodynamic forces. Although studies do not show a clear consensus on the optimal overlap of the rotor halves, values of 15 % to 30 % of the cylinder diameter (chord) have been reported to maximize performance[21]. Due their reliance on drag from the wind for torque, Savonius rotors operate at a tip speed ratio no greater than 1.0 to 1.4. Maximum efficiency occurs at a tip speed ratio in the range of 0.4 to 0.7 with a coefficient of performance of around 0.15. However, performance rapidly drops for tip speed ratios above and below the optimum value, requiring careful matching of the rotor, generator, and load. Advantages of Savonius wind turbines include the ability to self-start, low cut-in speed, no need for a yaw mechanism, small footprint, and simple construction[22].

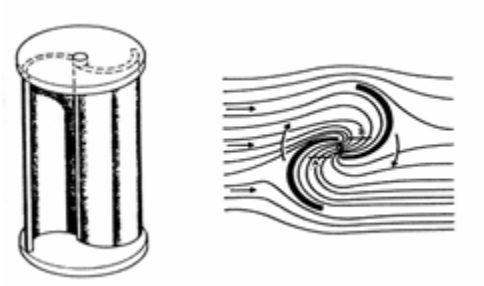

Figure 3: Typical Savonius rotor and streamlines around rotor cross section[23].

2.10 Hybrid

A hybrid design is a mixture of the Darrieus and the Savonius designs in order to take advantage of each of their benefits. The Darrieus design has a high power coefficient and is typically more efficient in comparison to other vertical axis designs, but it is not capable of self-starting. The Savonius design has a high starting torque and is capable of self-starting but its rotational speed and power coefficient are low. The aim of hybrid designs is to create a rotor that

combines the advantages of the Darrieus and the Savonius, making it capable of self-starting, producing a high starting torque and improved efficiency.

A Ropatec WRE.060 model, as seen in Figure 4, is an example of a hybrid design. The Ropatec has two asymmetrical airfoils along the sides, allowing for lift force to rotate the blades and center panel that redirects the air towards the airfoils[12]. It has a cut in speed of about 2m/s and it can reach its optimal power output at 14m/s[12]. Unlike most turbine designs that require the turbine to shut down at certain wind speeds, the Ropatec turbine is designed to have a braking effect making it stall at high wind since it is rated to produce power in wind speeds as high as 63m/s[12].

Figure 4: Ropatec WRE.060 model[12]

Other examples of hybrid turbines are the helical and the turby wind turbines. The helical design is made to be aesthetically pleasing and for high wind speeds. For example, the Windside Wind Turbine can be used up in wind speeds of 60 m/s. Turby turbines are designed to decrease the negative effects commonly associated with the Darrieus design, such as vibrations, high noise levels and low efficiency, by using three twisted blades the change of the angle of attack is more gradual[12]. An example of each of these turbines can be seen in Figure 5.

Figure 5: Windside Wind Turbine (left). Turby triple blade turbine (right)[12]

2.11 Electricity Generation Methods

Motors are typically used to convert electrical power to mechanical power, but when motors are supplied with mechanical power they function as generators producing electricity. In wind turbines, the mechanical power from the wind rotating the blades rotates the shaft in the generator to produce electricity. The maintenance and cost of the motor, and application of the electricity dictates whether a motor that generates alternating current (AC) or direct current (DC) is used. DC motors are not typically used for large wind turbines because the current used in households is already AC and the motor has high maintenance and production cost[23]. For small wind turbines, AC or DC generators can both be used but DC generators are typically used to charge batteries.

There are two main types of AC generators used to generate electricity by electromagnetic induction: synchronous and asynchronous. Synchronous motors generate electricity using a stator, a rotor and armature coils. The stator has AC current running through it

and creates a rotating EMF. The rotor is powered using DC current to create its own magnetic field. The rotor's EMF is attracted to its opposite pole on the rotating EMF, inducing the rotor to rotate at the same speed or synchronous with the rotating magnetic field[23]. However, if there is no rotation on the rotor, the rotor will not be able to spin due to the torque required to turn it. In asynchronous generators (also known as induction or squirrel cage generators) electricity is inducted in the rotor rather than through direct electric connection. When AC current passes through the stator winding, a rotating electromagnetic field is produced. Current is induced in the bars of the squirrel cage, which produces a force that makes the cage rotate. This type of motor primarily produces electricity through the difference in rotational speed between the magnetic field and the cage[23]. As the cage's rotational speed slows down, the rotor will experience oscillation between the north and south poles from the rotating magnetic field. This difference will cause more current to be produced and the force generated will make the cage rotate faster. This will continuously happen because the rotor is asynchronous and spinning slower than the rotating magnetic field[23]. While it appears that this type of generator can produce electricity, it must always be supplied with current to maintain its magnetic field.

DC generators produce an internal alternating current that is converted to direct current before the output terminals. For small DC generators, the coils are typically wound on the rotor which rotates inside two stationary permanent magnets. As with AC generators, an internal alternating voltage is induced in the windings by a rotating magnetic field which subjects the windings to alternating north and south magnetic poles. This voltage is applied to the output terminals using two brushes that complete the circuit through a segmented conductor known as a commutator[24]. The commutator reverses the negative half of the AC signal so that only a positive pulsating voltage is produced, as can be seen in Figure 6[25]. This pulsating voltage can

be evened out to create an approximately constant voltage by increasing the number of coils or poles on the rotor, which in turn results in an approximately constant current when the terminals are connected to a load.

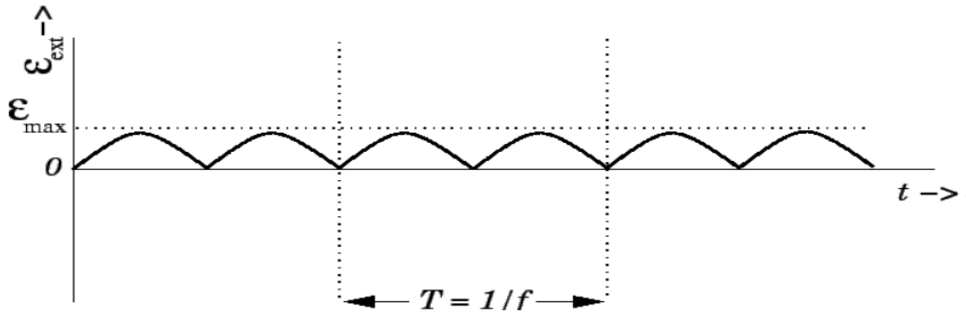

Figure 6: EMF produced by a DC generator[27]

Since DC generators are no longer widely produced due to the high complexity and low reliability of the brushes and commutator, it is practical to repurpose DC motors as a substitute. While no modifications to the motors are required to use them as generators, a motor with the appropriate: voltage, current, and torque characteristics must be selected in order to produce the desired power for a given input torque and RPM. When operated as generators, DC motors have an initial torque called starting torque that must be overcome in order for the shaft of the motor to rotate. At free run, where there is no torque, the motor will run at the maximum RPM and produce the minimum amount of current. When the motor runs at half of the maximum RPM

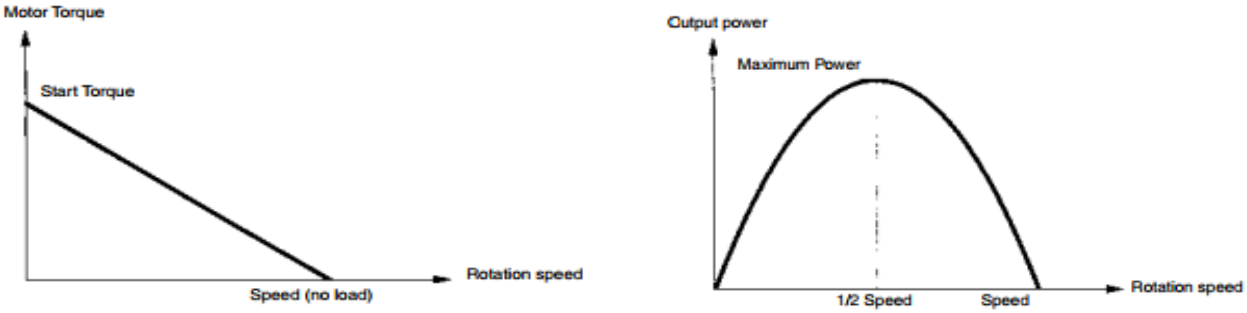

Figure 7: Plot of relationship between torque on the motor and rotational speed(left) and plot of power changing with respect to the rotational speed of the motor(right)[28].

with no load, it will produce the maximum power. Figures 7, and 8 show the relationships between RPM, torque and current[26].

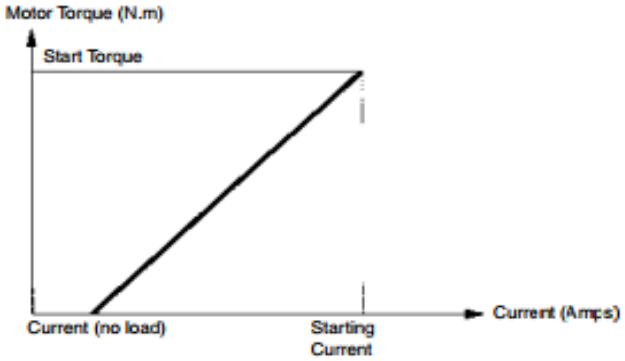

Figure 8: Plot of the relationship between torque on the motor and the current produced[28].

Motors are rated for certain operating limits, and exceeding them would damage the motor mechanically and thermally. Figure 9 shows a general curve of a DC motor and shows that the rated operating of a motor is about 25 percent of the stall torque and is less than the maximum efficiency[27].

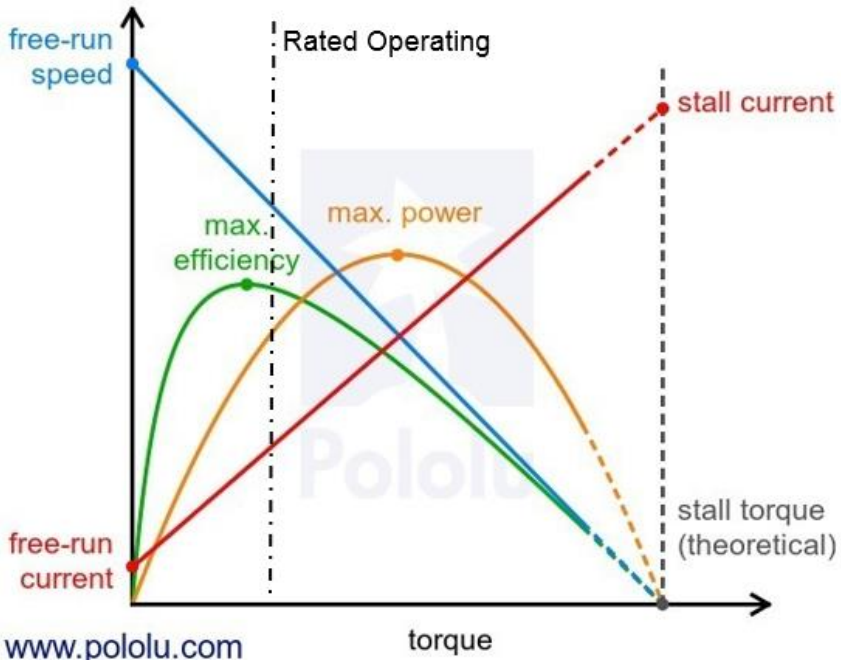

Figure 9: Graph showing the power, efficiency, RPM and current in relation to torque[29].

3. Methodology

The goal of this project is to develop a design for a cheap but effective wind turbine that can be built using recycled materials. The turbine must have a cut-in speed no greater than 5 m/s, produce at least 8 watts, and be created from at least 75% recycled material. The design must also be repeatable by someone with only moderate technical skills. This allows our project to reach our target demographic of off-grid communities, developing countries, or areas recently affected by natural disasters. To meet these objectives we identified the following tasks to be completed:

- Select turbine type
- Develop and optimize the blade design
- Select Motor
- Develop method for testing the turbine's performance
- Construct turbine from components
- Test the turbine
- Develop future recommendations

3.1 Design Section

3.1.1 Selection of Turbine Type

The first step in the design process was to determine whether a vertical axis turbine (VAWT) or a horizontal axis turbine (HAWT) best suited our application. To do this, we compared typical torque, tip speed ratio, coefficient of power, and cut-in speed values for each design. We also looked into previous at home DIY turbine designs as well to see whether one

type of turbine required less skill to create or if one type performed better than the other. From our research we determined that both types of turbines have their own sets of advantages and disadvantages; however, in the end it was decided that a vertical axis turbine would best suit our needs.

Table 1: Comparison of characteristics between HAWT and VAWT

Characteristic	HAWT	VAWT
Tip Speed Ratio	6	<1 to 3
Torque Output	Low Torque High RPM	High torque Low RPM
Cut-in Speed	5 m/s	2 m/s to 5 m/s
Coefficient of Power	~0.40	0.15 to 0.4
Yaw System	Requires Yaw System	Does not Require Yaw System

Based upon our findings, as seen in Table 1, we concluded that a Vertical Axis Turbine best suited our design application. This decision was made for a variety of reasons. First, we wanted our turbine to produce electricity in low wind conditions (wind velocities between 5-10 knots or 2.6-5.14m/s). This would require the turbine to produce enough torque to spin the motor. Vertical axis turbines are best suited for these conditions because they can have cut-in speeds at the low end of our desired range. They also typically produce larger amounts of torque which would allow our motor shaft to spin and generate electricity. Second, our design needed to be low tech. Horizontal axis turbines only generate power if they are facing the wind. This means a yaw system is required to keep the turbine pointed in the correct direction. Developing this system would require additional steps in the design process and would make the turbine more complicated to manufacture. Vertical axis turbines, however, are unidirectional and do not require a yaw system, which makes them easier to manufacture. Selecting a vertical axis turbine

did come with some drawbacks. By forgoing the horizontal axis turbine design we sacrificed efficiency and tip speed ratio. Horizontal axis turbines are typically more efficient than vertical axis turbines and they operate at higher tip speed ratios. This means that for a given wind speed the main shaft rotates faster and produces more electricity.

Once we chose to construct a vertical axis turbine, the next step was to determine which model best suited our application. From our research we identified three potential models: Darrieus, Savonius, or Hybrid. In order to pick the best design, we compared the characteristics of each model to determine which one best suited our intended design criteria. The comparison can be seen in Table 2.

Table 2: Comparison of Darrieus, Savonius, and Hybrid VAWT designs

Characteristic	Darrieus	Savonius	Hybrid (Ropatec)
Number of Blades	2-3	2	4
Tip Speed Ratio	2 to 4	0.4 to 0.7	N/A
Coefficient of Power	0.3 to 0.4	0.15	N/A
Self-Starting	No	Yes	Yes
Construction Concerns	Curved egg-beater blades could be difficult to manufacture	Simple to construct; blades provide structural support	Simple but many blades and center panels requires time to build,
Additional Information	Self regulates speed. once started remains at most efficient TSR	Not suitable for electric power generation due to low operating RPM	Nominal output at wind speeds of 14 m/s and greater

We concluded that the Savonius model was a poor choice for our application. While Savonius turbines are self-starting, easy to construct, and have low cut-in speeds, the tip speed ratio was too low[21]. With this turbine design we would be unable to generate sufficient amounts of electricity. The Darrieus turbine was a potential candidate because it had high efficiencies and was self-regulating in speed[18]. The curvature in the blades helped the turbine

operate at the most efficient tip speed ratio even when the wind increased. However, Darrieus turbines are not self-starting, which means it would need to be started manually. For the purposes of testing this was not a significant issue, but for someone constructing the turbine to generate electricity in real life, this could be a serious design flaw. Additionally, the curvature in the blades was unappealing because the required curved airfoil profile would be difficult to manufacture. Since our target audience was DIYer's with only moderate technical skills, the curved blade geometry could potentially be too complicated. It could also require a material not readily available to the everyday consumer. This left the hybrid design. This design proved most promising because it combined features from both the Savonius and Darrieus turbines. Hybrid turbines can self-start like Savonius, but they typically operate at the higher tip speed ratios and efficiencies of the Darrieus turbines. Another benefit of this design is that hybrids can have more than two blades, whereas Darrieus and Savonius typically do not. Additional blades are advantageous because the turbine is more balanced, and the transition between positive and negative angles of attack is more gradual, which reduces vibration.

3.1.2 Development and Optimization of the Blade Design

In order to begin designing the system we needed to understand the amount of power and torque we could generate given our design constraints. This would help us determine not only the type of motor we needed, but also the overall size, and type of turbine that was most optimal to use. To begin the process, we created power and torque curves in MATLAB for horizontal axis turbines with radii of 0.5, 1, 1.5 and 2 meters respectively. For the purpose of this simulation we assumed the turbines operated at a TSR of six and a coefficient of power for the turbine of 20%. We chose a TSR of six because the recommended tip speed ratio for commercial turbines is

between six and eight[10]. Six was a conservative estimate as it was on the low end of the range of recommended tip speed ratios[10], [11].

Given that we are constructing a small scale turbine from repurposed materials, it is likely that the system will be relatively inefficient. We chose our turbine's coefficient of performance to be 20% since it is approximately half the coefficient of performance for a typical commercial turbine This was an optimistic estimate for our turbine, but still fairly conservative.[30]. We then substituted these variables into equations 4, 5, and 6 for wind speeds ranging from 0 to 9 m/s in increments of 9/1000 m/s.

$$(4) \qquad P = \frac{1}{2}\rho A_{swept} C_p U_{inf}^3$$

$$(5) \qquad \omega = \frac{\lambda U_{inf}}{R}$$

$$(6) \qquad T = \frac{P}{\omega}$$

Figures 10 and 11 show results for power versus wind speed and torque versus wind speed for the various radii respectively. We then analyzed the plots to determine which size radius would provide us with enough torque to spin the shaft of a generator while providing us with sufficient power to satisfy our energy design criteria. The results from this simulation confirmed our decision against selecting a HAWT. Since we were designing a turbine to operate in low wind conditions, both cut-in speed and torque production were key features. While the simulation illustrated that a HAWT would exceed our design power of 8 watts, the torque output at low wind speeds was a point of concern. Storage space for the turbine when it was not in operation was limited, which meant we had to keep the total size of the turbine to a minimum. At the desired cut-in speed of 2.5 m/s a turbine with a radius of 1.5m would only generate

approximately 6 Newton-meters of torque and a turbine with a 1m radius only generated approximately 2 Newton-meters of torque. As seen from the gearing ratio section, 2 Newton-Meters would not be sufficient to spin the motor at the desired cut-in speed. Therefore, if we went with a HAWT we would have to either increase the cut-in speed or go with a larger turbine. However, increasing the size was not a practical option. Larger blades would require more materials, which would make the turbine more expensive and difficult to manufacture. Additionally, it would require additional storage space, which we did not have readily available to us, this information combined with the other drawbacks associated with HAWTs lead us to look into a VAWT design.

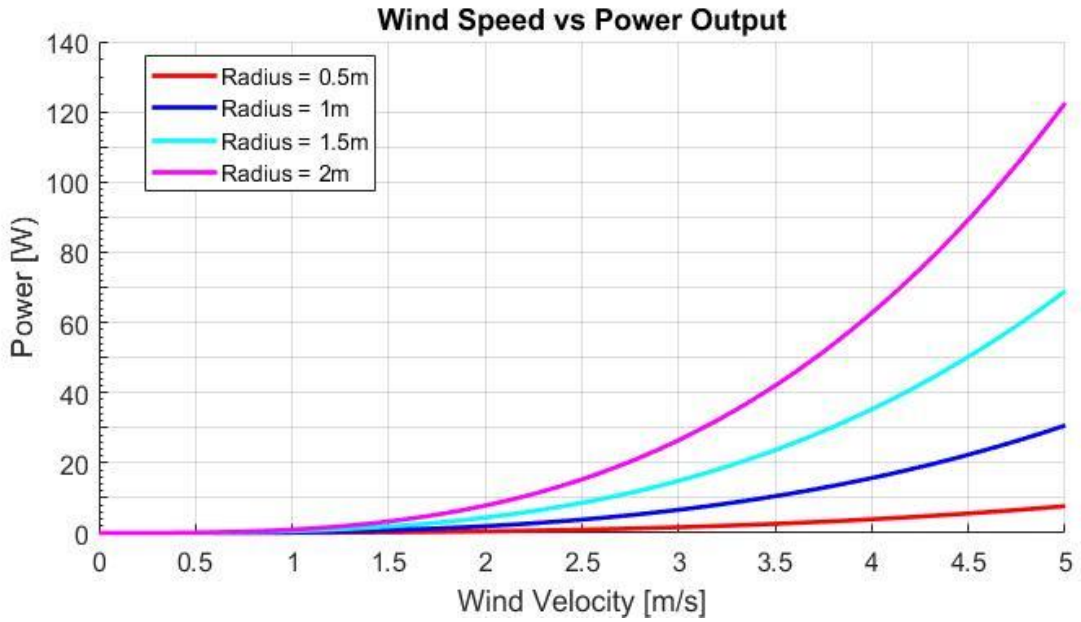

Figure 10: Power versus wind velocity for a HAWT

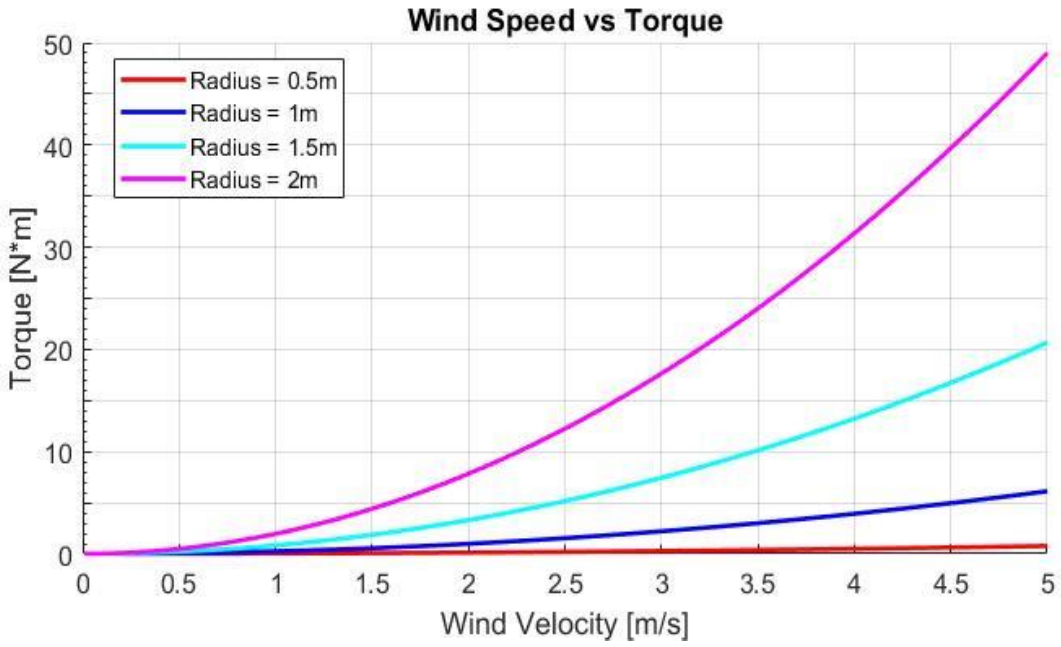

Figure 11: Plot of Torque versus wind velocity for HAWT

We then modified our simulation to accommodate the specifications of a VAWT to verify that one would provide sufficient power and torque for our application. Because VAWTs typically operate at slower speeds than HAWTs, we changed the TSR from six to one. Even though we had identified that either a Darrieus or Hybrid design, which both operate at TSR greater than one, we selected a TSR of one for this simulation because it was a conservative estimate. Underestimating the performance of our turbine would help ensure that the turbine size we selected would provide sufficient amounts of power and torque to spin the motor we selected. The second change we made to the simulation was the calculation used to calculate the turbines' swept area. For a HAWT, swept area can be calculated by the area of a circle with a radius equal to the length of the blades, as seen in equation 7. However, because the axis of rotation for a VAWT is rotated 90 degrees from that of a HAWT, this equation does not accurately reflect the swept area for a VAWT. The swept area of a VAWT is calculated by the area of a rectangle with

a width equal to the diameter of the rotor and a height equal to the height of the blades, as seen in Equation 8.

$$(7)\ A_{swept} = \pi(length\ of\ blade)^2$$

$$(8)\ \ A_{swept} = 2(Blade\ Height)(Blade\ Radius)$$

We then substituted these modifications into the HAWT simulation to generate plots of power versus wind speed and torque versus wind speed for turbines with heights of 1, 2, 3, and 4 meters and radius increments of 0.5, 1, 1.5, and 2 meters. The plots of power versus wind speed can be seen in Appendix A and plots of torque versus wind speed can be seen in Appendix B. Ultimately, the size constraints of our storage facility proved to be the most limiting factor in our design selection process. The 3 and 4 meter tall turbines were impractical, even though they did provide high amounts of torque at the low wind speeds we desired. The 2 and 1.5 meter radii were also eliminated for similar reasons. This left us with the option of choosing between a blade height of 1 or 2 meter and a radius of 0.5 or 1 meter. Once again, the size constraint was the most limiting factor. While we could have stored the 2m tall turbine, manufacturing a blade that long would have limited our potential construction materials. Therefore, we decided that a 1m height was most practical. The next design decision was determining the blade radius. Smaller blade radius correlated with a higher main shaft RPM; however, this meant the blade would produce less torque. As illustrated in Table 3, the 1m blade radius only doubled a potential gearing ratio, but resulted in a significant increase in torque production. We ultimately decided that the 1m blade radius was the most advantageous. The turbine we ultimately chose had a height and radius of 1m.

Table 3: Required gearing ratios for various sized radius and tower heights for VAWTs (300 RPMs chosen based upon motor selection as described in the Motor Selection Section).

Turbine Height (m)	Turbine Radius (m)	Wind Speed (m/s)	Power Output (W)	Omega (RPM)	Gearing Ratio to 300 RPM
1	0.5	2.5	1	47.75	6.3
		5.1	8	95.5	3.1
	1	2.5	2	23.89	12.6
		4	8	38.2	7.9
2	0.5	2.5	1.8	47.75	6.3
		4	8	76.4	3.9
	1	2.5	3.8	23.88	12.6
		3.15	8	48.7	6.2

3.1.3 Optimization of blade aspect ratios

Once a turbine design and approximate size was chosen, the next step in the design process was optimizing the relative dimensions of the turbine: aspect ratio of the blades (H/c) and the height to diameter ratio (H/D). The objective of this optimization was to maximize the efficiency of the turbine for our design wind speed of 4 m/s. Using our previously selected turbine radius, the ratios would then provide us with the dimensions for the blade height, chord length and turbine radius. In order to determine the optimal ratios for a given wind speed, an efficiency curve (Cp vs. TSR) must be generated for a range of turbines with varying dimensions.

According to a study by Alessandro Bianchini, Giovanni Ferrara, and Lorenzo Ferrari on the optimization of H-Rotor turbines, optimal turbine dimensions can be determined given a wind speed, swept area and airfoil shape. Bianchini et al. used the VARDAR program from the University of Florence to maximize annual energy yield for a given turbine. The VARDAR

program uses a modified blade element momentum theory program that incorporated the Double Multiple Streamtube Approach with Variable Interference Factors to calculate power output for a given wind speed distribution, and turbine dimensions[28].

For our turbine, we assumed a wind speed distribution with an average of 3 m/s since it is comparable to the average wind speed in Worcester, and a swept area of 1 m^2 since it was nearest to our desired turbine size. For a turbine with the previously mentioned parameters and a NACA 0018 blade airfoil, the results from this study give an H/D ratio of 0.4, a c/D ratio of 0.185, and a blade aspect ratio (H/c) of 2.2[28]. Using our previously chosen turbine radius of 1 m, the remaining dimensions could then be determined, giving a height of 0.8 m and a chord length of 0.37 m. These dimensions and the ratios used to find them are summarized in Table 4.

Table 4: Optimal turbine dimension ratios and actual dimension lengths

Dimension Ratio	Optimal Value	Dimension	Length [m]
H/D	0.4	Diameter	2
c/D	0.185	Blade Height	0.8
H/c	2.2	Chord length	0.37

3.1.5 Material selection and initial design

Once the turbine design constraints were identified, the next step in the design process was selecting materials and developing an initial design. Because our turbine needed to be producible in off-grid locations or areas recently affected by natural disasters, we were presented with some unique design challenges. First, we had to limit the number of custom machined parts so that someone with moderate technical skills and a limited set of tools could still manufacture the turbine. Second, we had to use materials that would either be readily available in the target locations, or could be purchased relatively easily. In order to satisfy these two constraints we

decided to construct the turbine out of materials that were either commonly used in construction or sold at local hardware stores.

3.1.5-A Tower construction

Given the dimensions of our turbine, and the weight of our motor we needed a sturdy tower base that would: support the weight of the blades and motor, remain stable during operation, and provide some elevation to the blades in order to improve airflow. We ultimately decided that constructing the tower from 0.75” black pipe was the best option given our design constraints. We chose this option because the pipes were strong enough to support the weight of the motor and blades with very minimal deflection (6.95mm at the operational wind velocity of 5 m/s). Black pipe is also readily available in most hardware stores with standard fittings that are easily attached. We chose the 0.75” diameter pipe because it has an outer diameter of approximately 1.05” which is the inner dimension of the roller bearings we selected. As can be seen in Figure 12 the tower consists of four legs attached to a central 6-way union, with a central shaft on top. The motor mount was located just above the 6-way union to help keep the center of gravity as low as possible. Additional legs were added to the motor in order to provide additional stability to the turbine and help further reduce the deflection of the main shaft to only 3.13mm. The deflection calculations can be found in Appendix C.

Figure 12: Turbine tower with motor mount

3.1.5-B Blade Construction

Darrieus Turbine blades are typically made to have a symmetrical NACA 0018 or NACA 0015 airfoil shape[18]. Based on the calculations to determine the optimal blade aspect ratio, we determined that our turbine should have blades with a height of 0.8m and a chord length of 0.3636m. Given that airfoils are precise shapes and that our target audience only has limited access to tools, we devised two blade designs, seen in Figure 13. One design was to be constructed out of foam with two central wooden spars for strength. The foam was then wrapped in marine-grade shrink wrap to protect the foam from the elements. The second design was to be constructed in a similar manner to a model airplane wing. It would have an inner skeleton created from plywood with two central wooden spars running through the middle for strength. The wooden frame would then be wrapped in the marine-grade shrink wrap to give the airfoil shape.

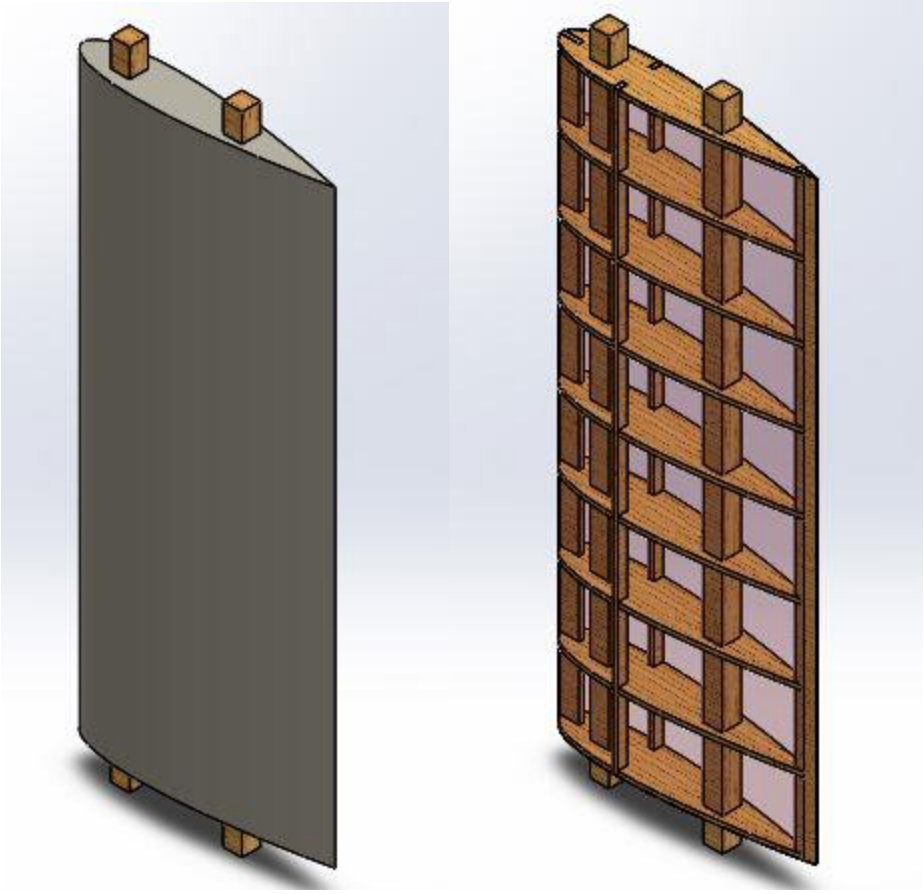

Figure 13: Foam blade assembly (left) and Wooden frame assembly (right)

Table 5: Pros and cons of the two blade designs

Foam Blade		Wooden Blade	
Pros	Cons	Pros	Cons
Lightweight	Time consuming without a hotwire to shape foam	Strong internal structure	Large parts list
Can be created without power tools	Could be difficult to manufacture exact airfoil shape	Can manufacture exact airfoil shape	Difficult to manufacture without power tools
Few parts to manufacture	Potentially weak structure in foam	Could be manufactured relatively quickly if using WPI's laser cutter	Shrink wrap over wooden ribs could pucker creating imperfect airfoil.

Given the benefits and drawbacks of each blade design we ultimately decided to use the foam blade design. We created the blade using 2” thick sheets of foam insulation and 0.75”x1” wooden posts purchased from Lowe’s. We then cut the foam into 0.3636m x 0.8m lengths. Using a hotwire we cut 0.375”x 1” notches in the foam to locate the center spars that were created from the wooden posts. We then glued the components together using insulation foam glue, and cut out the blade profile using a hotwire; however, if we did not have electricity the foam could have been shaped using wire brushes and sandpaper.

3.1.5-C Outer Shaft Construction

The turbine blade assembly was connected to the tower through an outer shaft that sat around two roller thrust bearings. This outer shaft was then broken down into 2 subsections: Main shaft, Figure 14 and the bearing housings, Figure 15. The main shaft was created using 2” plastic PVC pipe. We chose 2” pipe because it was relatively stiff and a standard size so it would fit over the outer edge of a roller thrust bearing. We chose 2” pipe because it was relatively stiff and a standard size so it would fit over the outer edge of a roller thrust bearing. As can be seen in appendix D, the maximum deflection of the outer shaft was $2.036*10^{-3}$ mm at the operational wind velocity of 5 m/s. The materials used to construct the main bearing assembly can be seen in Table 6 and the materials used to construct the main shaft can be found in Table 7.

Table 6: Materials used in construction of main bearing assembly

Part Name	Material	Exploded View Part Number
Sioux Chief 2” Shower Drain	PVC	1
Bearing	Roller thrust Bearing	2
Central Blade Attachment Flange	¼” Aluminum Sheet	3
Bearing Mount	PVC Cutout From Shower Drain	4
Bearing Mount Housing	PVC Cutout From Shower Drain	5

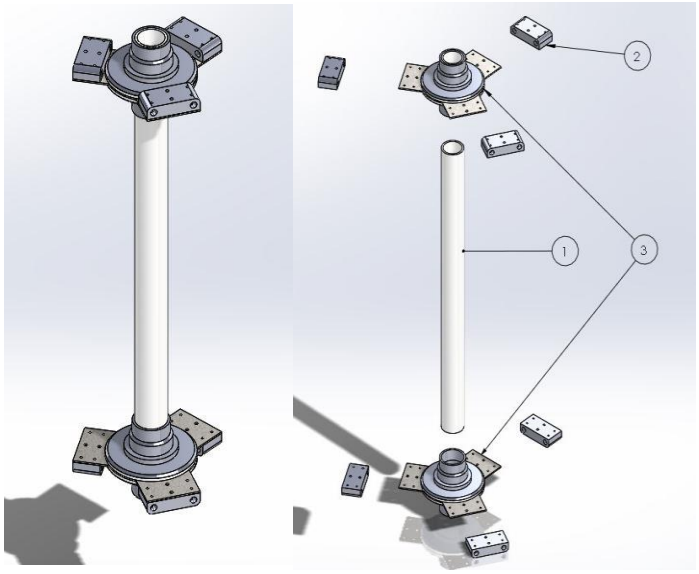

Figure 14: Outer shaft assembly (left) and exploded view of outer shaft assembly (right)

Table 7: Materials used in construction of Main Shaft Assembly

Part name	Material	Exploded View Part Number
Main Shaft	2” PVC Pipe	1
Blade Attachment Bracket	2” x 4” x 1” Aluminum	2
Main Bearing Assembly	N/A	3

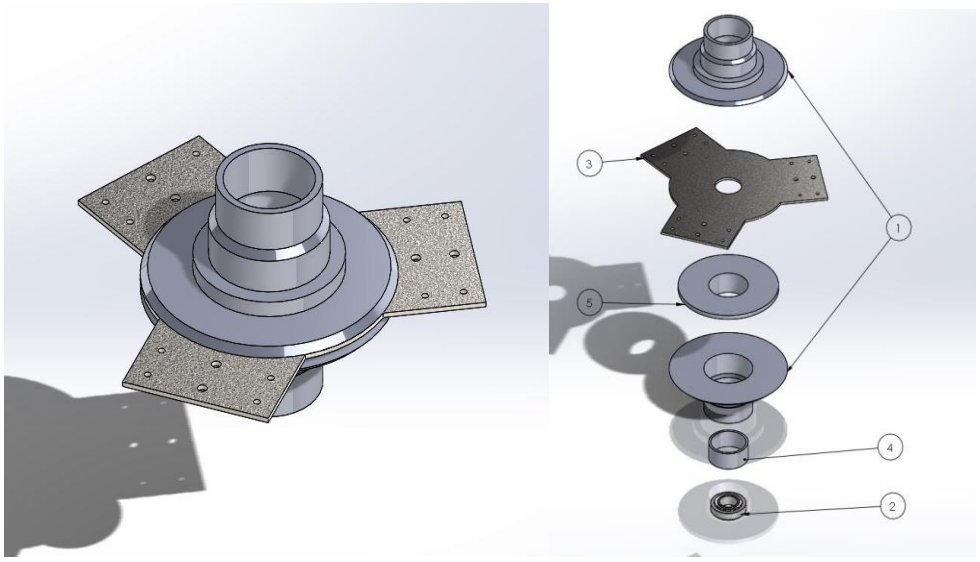

Figure 15: Main bearing assembly (left) and exploded view of bearing assembly (right)

3.1.5-D Mounting Brackets and Blade arms

Connecting the blades to the central shaft proved most difficult. Given our design constraints we could not design complicated, custom brackets that required extensive machining such as milling, or welding. Consequently, we developed a method that required minimal amount of machining and minimal steps. The system, depicted in Figure 16, consisted of a mounting bracket and two blade arms that connected to the blades. The mounting block was attached to the central mounting bracket on the outer shaft. One side of the blade arm were attached to the mounting block via two #8 machine screws. The other side of the blade arm was connected to the blade itself via holes located in the wooden spars. The blade arms were then secured with two cotter pins. Two arms were used in order to minimize any torsional rotation caused by the shaft. From this attachment system we were able to develop two similar designs which can be seen in Table 8. Initially, the lower profile of design 1, seen in Figure 17 (left), made it most appealing. However, the lower profile required us to construct the blade arms from solid 0.25" threaded rods which were heavier than the hollow 0.5" rods used in the second design, Figure 17 (right).

Table 8: Dimension and materials of mounting bracket and blade arm assembly

Component	Design 1		Design 2	
	Material	Dimensions	Material	Dimension
Blade arms	Stainless Steel Threaded Rod	3'x 0.25"-20	Stainless Steel Conduit	0.5"x 3'
Mounting Bracket	Aluminum Bar Stock	2" x 1.75" x 0.25"	Aluminum Bar stock	4" x 2" x 1"
Blade Arms Attachment Method	0.25" Stainless Steel Nuts	Attached to either end of the mounting bracket	# 8-32 x 1.25" Stainless Steel Machine Screws	Mounted through the mounting bracket and blade arm

Table 9: Pros and cons of the two mounting bracket and blade arm assemblies

Design 1		Design 2	
Pros	Cons	Pros	Cons
Lightest of the wo designs	Blade arms are heavy	Larger moment means less torsional rotation	Larger Profile
Lowest Profile	Smaller moment more likely to permit torsional rotation	Blade arms are lighter	More material makes mounting brackets heavier
Can adjust blade arm length	Nuts could loosen up on blade arms	Less steps required to attach blade arms	

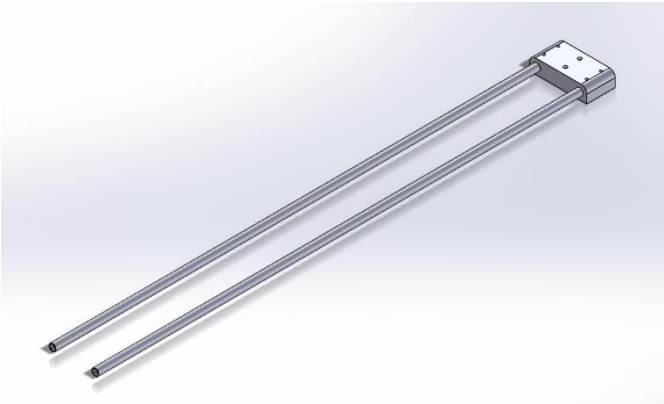

Figure 16: Image of mounting bracket and blade arms design two

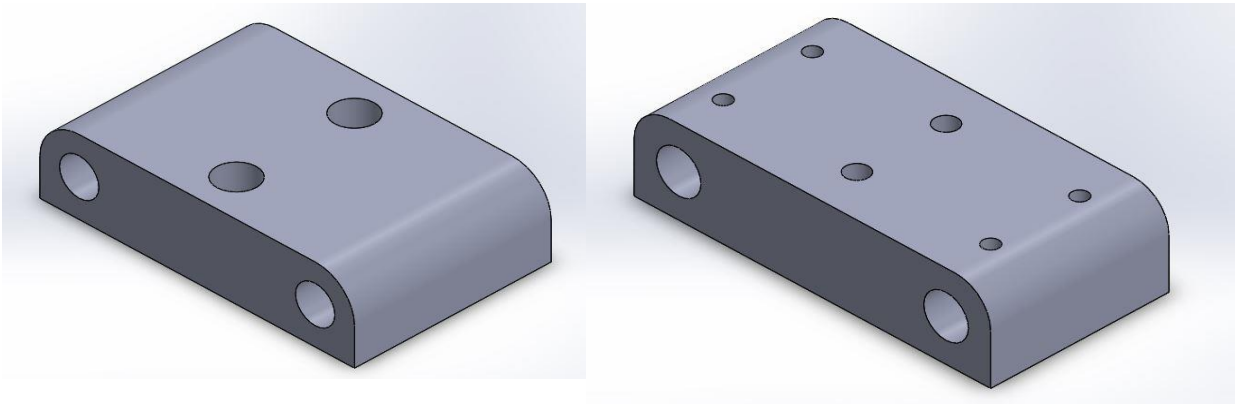

Figure 17: Mounting block design 1 (left) and Mounting block design 2 (right)

3.1.4 Motor Selection

In order to determine which generator will match the torque and rotational speed of our turbine we first determined which type of generator to use. AC generators are typically used for large-scale turbines but are not suited for small scale unless the electricity produced will power a house or is sent to the grid. DC generators are typically used for small scale and can be used to directly charge batteries, making it the best choice for our turbine.

We were able to find some motors that were capable of meeting the requirements for our turbine. We needed a motor that produces DC current, produces high voltage at low RPMs and has a low starting torque. Additionally, in order to successfully charge batteries, the motor needed to produce a voltage greater than the cell voltage of the selected battery. By having a low starting torque, we can have a gearing ratio which will allow us to increase the RPM of the motor, produce more power and increase the voltage produced by the motor. Table 10 compares the different characteristics of each motor we found.

Table 10: Comparison of the DC motors compatible with our turbine

Motor	WindZilla 12/24V	WindStream	Ametek 30V
RPM to produce 12V (Open circuit)	540	434	300
Starting Torque	Low but not specified	0.044 N-m	Low but not specified
Cost	$115	$300	$100-$200
Additional Information	Company provides some test data but no information found on actual use in wind turbines	Large size (8 in) and weight (9 lb); Maximum 3 Amp continuous current	It is well known and highly recommended among hobbyists as a wind turbine generator

Based on the motors found, we chose a tape drive motor since it had worked on previous wind turbine designs and it met our requirements while being cost effective. Tape drive motors, once used in large mainframe computers, produce an adequate DC voltage at a low speed on the order of a few hundred RPMs. They have been used by hobbyists as generators for 3 to 4 foot diameter HAWTs to produce a maximum power output of around 150 W. Although their power output is somewhat high for our application, the power output decreases for lower speeds and the motors produces an open circuit voltage of 37 V per 1000 RPM. This corresponds to an open circuit voltage of 12 V at about 300 RPM, which is within our operating range. It has a shaft of ⅝ inch diameter and 1 ⅞ inch long, which allows space for attaching a gear or pulley if necessary. The tape motor shown in Figure 18 is the Ametek #965922-102, rated for 37V at 900 RPM and was bought for $75 from a surplus store. We found that the starting torque was 0.02 N-m by attaching a lever to the shaft of the motor and applying small weights until the shaft started to rotate.

Figure 18: Ametek motor to be used for our turbine

3.1.4-A Finding voltage constant

In order to find the voltage produced by our generator at any given rotational speed, we needed to determine the voltage constant. We did this by driving the shaft of our generator with a similar DC motor and measuring the open circuit voltage for various rotational speeds, as seen in Figure 19.

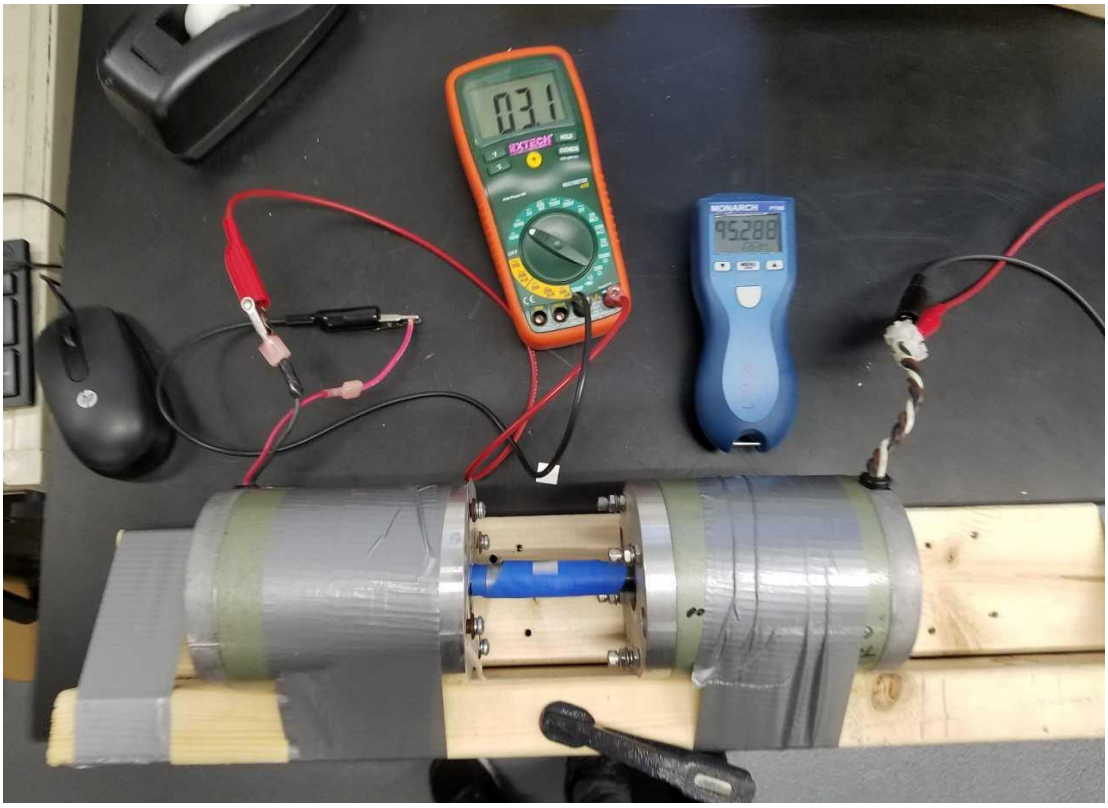

Figure 19: Setup of the experiment to measure the internal resistance.

We first taped the motors to blocks of wood to prevent any slippage or rotation of the motors themselves. We then clamped the wood to the table to prevent the motor setup from moving. Next, the two shafts were taped together with duct tape and then layered with blue masking tape to reduce reflection and minimize interference with the tachometer. The driving motor on the right was powered using a DC power supply in order to spin both motors at a constant rotational speed. Our motor, on the left, would then act as a generator so we could measure the output voltage using a voltmeter. With no load applied, we measured the voltage

generated and the rotational speed of our motor at various speeds using a volt meter and tachometer. We then used the measured voltage and RPM values to calculate the voltage constant for our motor (K_e). We determined K_e was 0.033V/RPM by averaging the V/RPM of our dataset.

3.1.4-B Internal Resistance of Motor

Motors have their own internal resistance which means that as they produce electricity there is some voltage drop. In order to find the internal resistance of our motor, we used the same setup used to find the voltage constant. We connected various resistances in series with the motor and measured the voltage drop across the resistors and the RPMs of the coupled motors.

$$(9) V_{out} = V_{in}\left(\frac{R_2}{R_1+R_2}\right)$$

Using Equation 9, also known as the voltage divider equation, we can find the internal resistance of our motor. The V_{in} which is the open circuit voltage of the generator, was calculated by multiplying the measured RPMs by K_e (voltage constant found previously). R_2 represents the resistor value used in the experiment, V_{out} is the measured voltage and R_1 is the unknown internal resistance of the motor. We were able to find that our motor had an internal resistance of 3Ω. Knowing the internal resistance will help us calculate the gear ratio needed for our turbine as well as determine the expected voltage output from the motor for a given load.

3.1.5 Selecting Gear Ratio

The appropriate drive train gear ratio was chosen by matching the mechanical power required by the generator with the power produced by the turbine at its maximum efficiency. However, first, we needed to know the turbine's maximum power coefficient (Cp) and the

corresponding tip speed ratio (TSR). This required developing a mathematical model to generate the Cp-TSR curve for our design wind speed. We attempted to write our own MATLAB script to implement the Multiple Streamtube Model developed by Strickland, but our program had difficulty converging on a solution and produced an unreasonable Cp-TSR curve[29]. However, we were able to find an open source MATLAB program, VAWT Analysis developed by Dietmar Rempfer and Peter Kozak, which uses the improved Double-Multiple Streamtube Model to determine the Cp-TSR curve[30]. Using the dimensions of our turbine, a free stream wind speed of 5 m/s, and Sheldahl and Klimas's aerodynamic data for the NACA 0018 airfoil at a Reynold's number of 180,000, the program produced the Cp-TSR curve shown in Figure 20. From this curve, the predicted maximum Cp is 0.28, which occurs at a TSR of three[31].

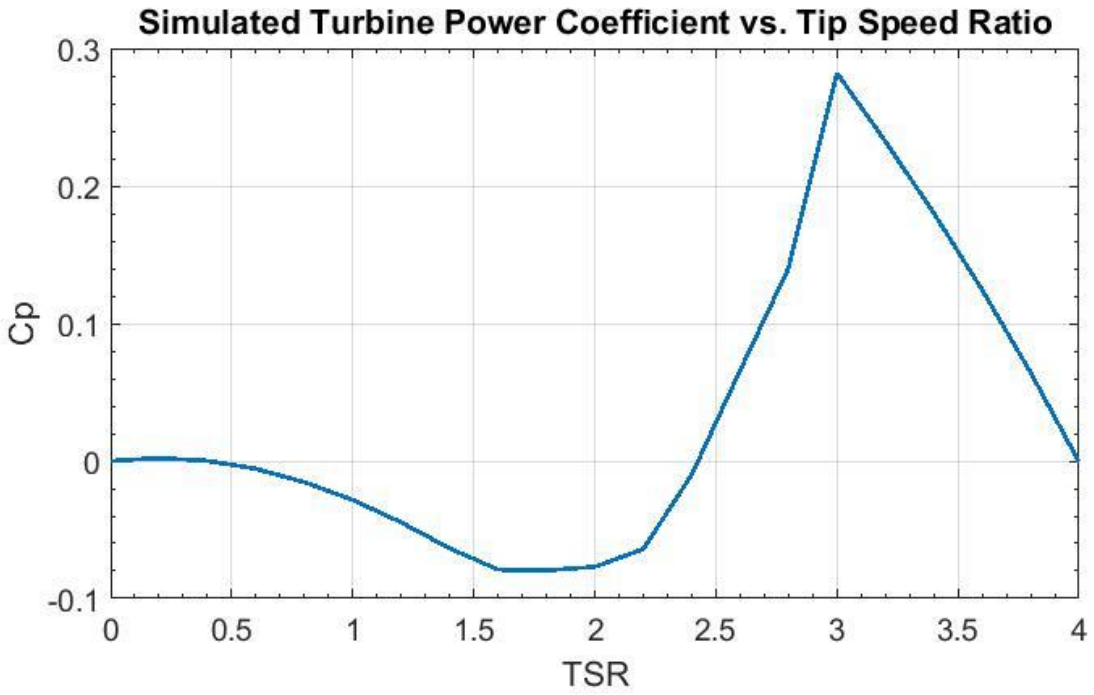

Figure 20: Predicted Cp vs. TSR curve using VAWT Analysis Matlab code

Using the equivalent circuit of a DC motor connected to a resistive load, we were able to find the torque required to spin the generator at a given RPM while accounting for the internal resistance of the generator and a resistive load. As seen in Equation 10, the torque required by

the generator is directly proportional to the current. The constant of proportionality, known as the torque constant, is related to the voltage constant by Equation 11. Based on the equivalent circuit of the generator and resistor, the current produced is given by Equation 12.

$$(10)\ T_g = K_T I$$

$$(11)\ K_T = K_e \frac{60}{2\pi}$$

$$(12)\ I = \frac{(K_e)(RPM_g)}{R_{internal}+R_{load}}$$

$$(13)\ RPM_g = \frac{60}{2\pi}\omega_g$$

$$(14)\ T_g = \frac{0.111\omega_g}{3+R_{load}}$$

By substituting Equations 11 through 13 into Equation 10, we were able to find Equation 14 which shows the relationship between the angular speed and the electrical load related to the torque specifically for our generator.

$$(15)\ T_g\omega_g = T_t\omega_t$$

$$(16)\ \left[0.0308\omega_g^2\right]_{generator} = \left[\frac{1}{2}C_p\rho V^3 A_{swept}\right]_{Turbine}$$

Assuming a load of 0.6 Ohms, we found that T_g is equal to $0.0308\omega_g$. Equation 16 was developed by substituting T_g and the turbine power output given by Equation 1 into Equation 15. The angular speed of the generator was then calculated using Equation 16. Given a resistive load

of 0.6 Ω, a wind velocity of 5 m/s, swept area of 1.6 m^2, Cp of 0.28, and an air density of 1.225kg/m^2, we calculated that ω_g was 33.3 radians per second which converts to 318 RPM.

$$(17)\ \omega_t = \frac{\lambda V}{R}$$

By substituting a value of 3 for the λ, 5m/s for V and 1m for R, we determined that our turbine rotational speed (ω_t) was 14.97 radians per second or 143 RPM. This means that a gearing ratio of 2.2 was needed to rotate the generator shaft at the desired 318 RPM.

$$(18)\ V_{out} = k_e RPM_g - IR_{internal}$$

Using Equation 12, we then calculated that the current produced when the generator was rotating at 318 RPM with a load of 0.6Ω was 2.9A. Using this current value and Equation 18, we calculated the output voltage of the loaded generator to be 1.75V. While this output voltage is lower than we anticipated, we could use a voltage booster (step-up converter) to increase the voltage needed to charge a battery. However this would decrease the amperage available for charging, which would make the charging process slower.

3.2 Testing Procedures

3.2.1 Testing Methods of Turbine Performance

In order to assess the performance characteristics of our turbine to determine whether it satisfied our design criteria, we performed multiple tests under windy conditions. Since WPI does not have a wind tunnel large enough for our turbine, all tests were conducted outdoors. With the unsteady nature of wind unavoidable in the test environment, it is important that

measurements are taken simultaneously when both the wind speed and turbine rotation are appear to be somewhat steady.

3.2.3 Procedure to test turbine electrical power output

To test the power output of the turbine, we set up the turbine on various windy days and recorded the voltage output of the generator, the turbine rotational speed, and the wind speed. To record the voltage we connected a resistor of 20 Ω in series with the generator and then connected multimeter across the resistor. The turbine rotational speed was measured using a non-contact tachometer directed at a strip of reflective tape attached to the turbine shaft. The wind speed was recorded using a handheld anemometer held at approximately the same height as the center of the turbine blades. We then simultaneously recorded the voltage, turbine RPMs, and wind velocity every 15 seconds when wind speed was strong enough to keep the turbine rotating. Using the data we collected, we calculated the power being output from the turbine using the equation 19 derived from Ohm's law.

$$(19)\ Power = \frac{V^2}{R}$$

4. Results

The data collected during the testing phase of this project illustrates that the development of a turbine from recycled and repurposed material is feasible. In general the turbine's performance was similar to the response predicted by our initial simulations. However, due to the assumptions made in the initial simulation and the limitations in the data collection process there are differences between the predicted turbine response and the actual values obtained from the turbine.

4.2 Turbine Rotational Speed

One of the main design parameters for this project was the rotational speed of the turbine. In order for the motor to generate enough power to actually charge an electric device, turbine had to spin the motor at a high enough RPM. As can be seen by Figure 21, our initial prediction, which had an assumed TSR of 1 and an overall efficiency of twenty percent, predicted that around the design wind speed of 5 m/s the turbine would spin at 47 RPM's.

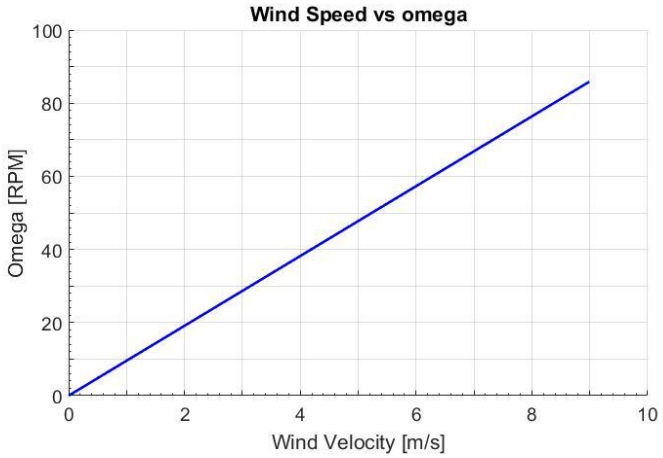

Figure 21: Plot of turbine angular velocity versus wind speed

As can be seen from Figure 22, the measured rotational speed increases with wind speed similar to the predicted response assuming a constant TSR. The slope of the trend line in Figure 23 corresponds to a TSR of 1.5. This suggests that lift, rather than drag, propelled the turbine blades faster than the wind speed. Since lift-based wind turbines are generally more efficient than drag-based turbines, this is a desired result.

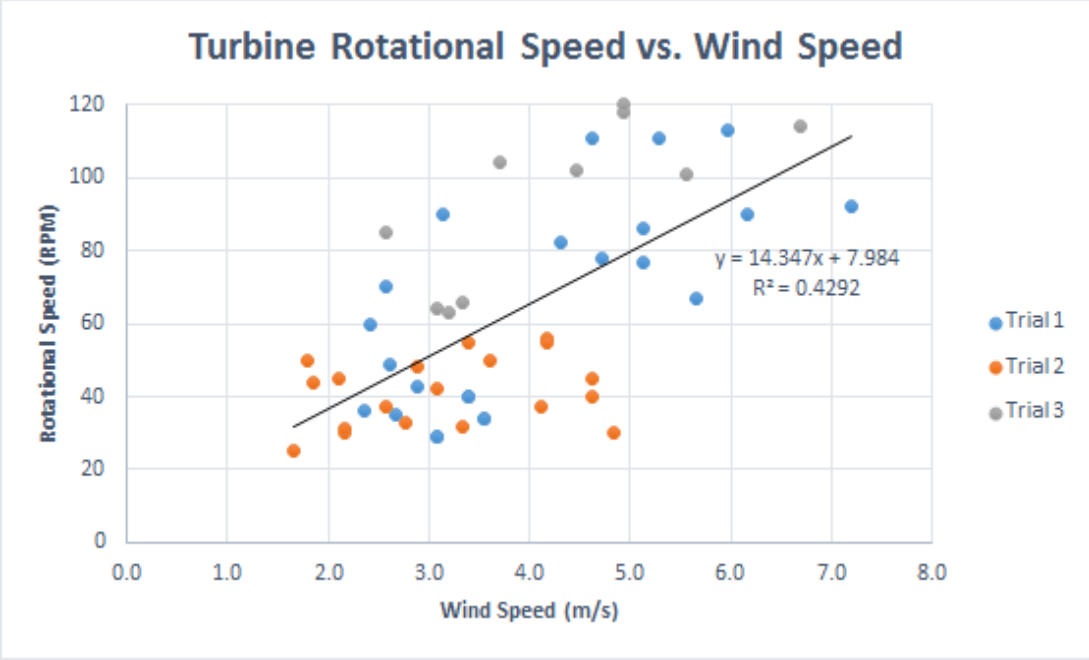

Figure 22: Measured turbine rotational speed at various wind speeds

The scatter of the points in Figure 22 is likely due to the accuracy of our wind measurements, the unsteadiness of the wind and the response time of our turbine to changes in wind speed. In particular, the reliability of the data from Trial 2 is questionable because the turbine RPM stays relatively constant despite a change in wind speed which is a different than what we observed in Trials 1 and 3. This may be a result of the especially turbulent wind which occurred during testing that day. Additionally, the relationship between turbine RPM and wind speed is not necessarily linear because it depends on the steady state balance of the torque produced by the blades and the various resistive torques acting on the turbine shaft. Since the

torques involved in this balance vary nonlinearly with wind speed and rotational speed, a control system would be required to ensure a constant TSR for all wind speeds and thus result in a linear relationship. As seen in Figure 23, the output voltage of the generator is linear with turbine rotational speed when connected to a resistive load. Since this linear dependence is expected for a permanent magnet DC generator, this plot was used to identify data points with obvious measurement errors. If a data point was significantly far from the trend line, it was removed from the entire data set in order reduce error.

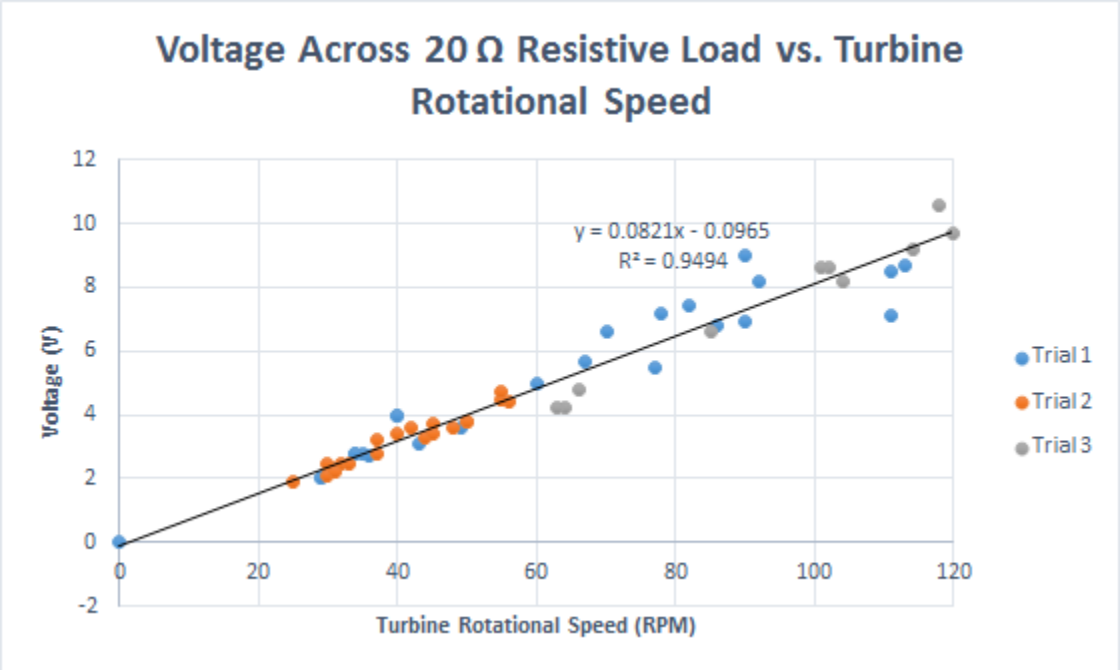

Figure 23: Measured generator voltage plotted against turbine rotational speed

Using an equivalent circuit consisting of the generator in series with the load resistor, the relationship between the expected voltage across the load and the turbine rotational speed is given by Equation 20, where V_L is the voltage across the load resistor, K_e is the generator voltage constant (0.033 Volts/RPM), R_{load} is the load resistance (20 Ohms), $R_{internal}$ is the internal resistance of the generator (3 Ohms), m_g is the gearing ratio of the generator and turbine pulley which is 2.9, and $N_{turbine}$ is the rotational speed of the turbine in RPMs.

$$(20)\ V_L = \left[\frac{K_e R_{load}}{R_{Internal}+R_{load}} m_G\right] N_{Turbine}$$

The slope of the trend line should then be approximately equal to the quantity in brackets (0.0832 Volts/RPM), which is reasonably close to the trend line slope of 0.0821 V/RPM. This suggests that our measured voltage and RPM data were accurate, with the exception of a few anomalous readings that were removed from the data set.

The electrical power output of the wind turbine was calculated from the voltage measured across the 20 Ohm load using Equation 19. The power output for each recorded wind speed can be seen in Figure 24. As expected, there is a positive correlation between the power and wind speed but due to the scatter in the data it is unclear how wind speed is related to the turbine's power output. Theoretically, the power output should increase with the cube of the wind speed; however, in actual turbines this relationship has also been observed to be approximately quadratic or linear. The scatter in Figure 25 is most likely due to the inaccuracy of our wind speed measurements. For example, at the design wind speed of 5 m/s, the data suggests that a power of 1.5 to 5.5 W was produced. It is likely that the lower range of these power values occurred at lower wind speeds than those actually recorded, and similarly the upper range likely occurred at higher wind speeds. As stated earlier, data from Trial 2 are likely inaccurate due to

the unsteadiness in the wind and the vortex effect from the surrounding buildings. Trials 1 and 3 likely give a more accurate indication of the turbine's power output.

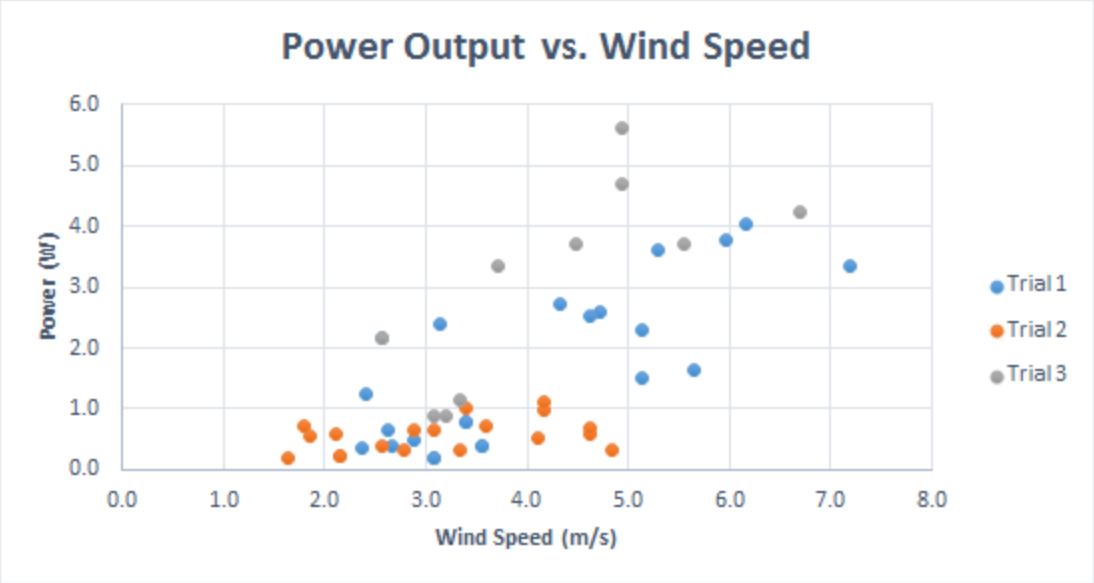

Figure 24: Electrical power output of generator plotted against measured wind speed

Typically, the performance of a wind turbine is given by a plot of its power coefficient as a function of tip speed ratio. Since we did not measure the mechanical power output of our wind turbine, we do not know the exact power coefficient of the turbine. However, the fraction of electrical power generated relative to the power available in the wind characterizes the overall efficiency of the wind turbine-generator system. System efficiency, a combination of the power coefficient, drive train efficiency, and generator efficiency, can be calculated by dividing the electrical power output of the generator by the power available in the wind. This value was plotted as a function of TSR in Figure 25. As expected the plot shows a positive trend in the efficiency, reaching a maximum efficiency of 13% at a TSR of 2.8. The theoretical maximum power coefficient for our turbine was predicted by the simulation to occur at a TSR of 3. While

our data seems to support this, we do not have any data from the higher TSRs, which makes it difficult to confirm that the maximum efficiency occurs at a TSR of 3. Further testing at higher wind speeds with higher resistance loads would indicate where the maximum efficiency occurs.

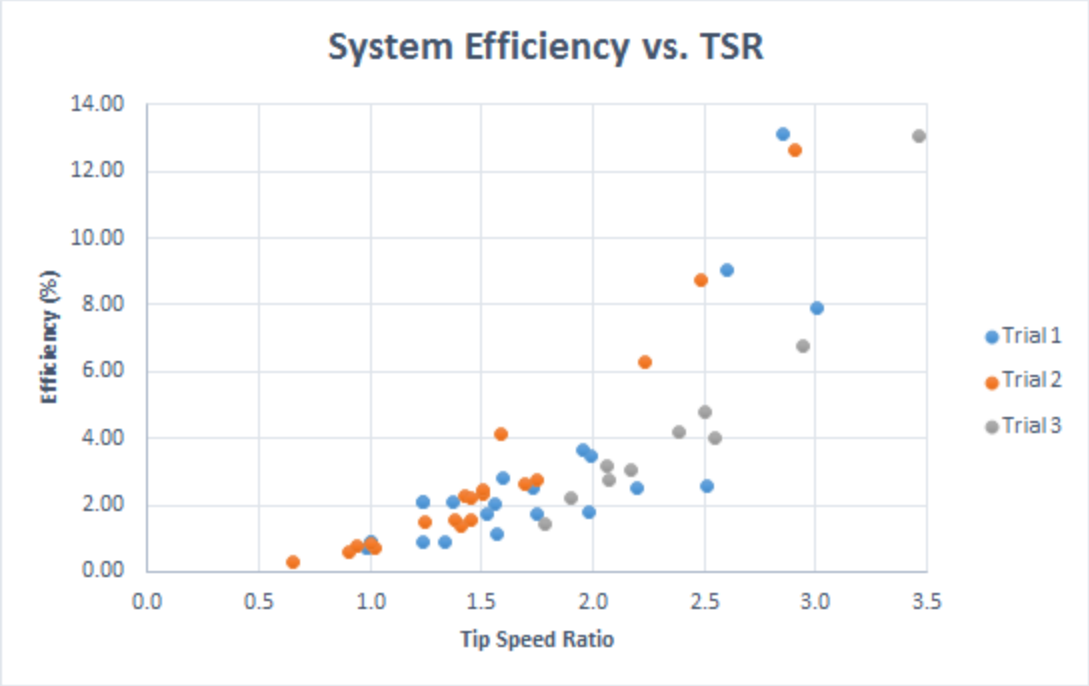

Figure 25: Overall system efficiency and tip speed ratio

4.3 Error in Data

4.3.1 Wind Speed

The main limitation of our project was the unpredictability of the wind and the testing location which made recording the wind speed difficult. Because of the turbine's size and the resources at WPI, we were unable to test in a controlled location such as a wind tunnel. Consequently, we were left with finding suitable locations to test outdoors on the WPI campus. Due to the weather conditions, much of our testing was done in the space between the Sports and Recreation center and the Park Avenue Parking Garage. We used this location to test because the

narrow space between the buildings created a funnel for the wind which artificially increased the wind velocity, giving us the speeds we desired. Unfortunately, this increased velocity was the result of the buildings disrupting the wind flow and generated vortices. This made collecting data on the wind velocity difficult for multiple reasons. First we were recording instantaneous wind velocities using a unidirectional handheld anemometer that was consistently held in one direction. However, because the buildings were creating vortices, the wind was actually constantly changing direction, thus making it nearly impossible to accurately record the wind velocity. Second, the wind measurements we recorded were phase shifted from the turbine's response, thus creating a margin of error between the recorded wind values and the power output from the turbine. The phase shift was caused by three factors: unpredictability of the gusts, initial time to spin the turbine up to speed, and the turbine's inertia. First, the gusts were random. They did not occur at regular intervals and lasted anywhere from 2-5 minutes in length. As result, we had no way to anticipate the onset of a gust and could only begin testing once the gust had begun. Second the turbine was not self-starting, which meant that the first 30-60 seconds of the gust could not be used to record data, creating a delay in the data collecting process. Third, the turbine's inertia kept the blades spinning at high RPMs even after the wind velocity had dropped. These three factors resulted in a mismatch between the wind velocities recorded and the performance of the turbine.

4.3.2 Turbine Rotational Speed

A laser tachometer measures RPM by counting the number of times per minute the laser is reflected off a special reflective sticker. During our testing, this worked most of the time, however there were some instances where the RPM values fluctuate between the actual value and values we knew were incorrect. We found that during the days we tested when the sun was

bright, we had more difficulties obtaining accurate values. One potential problem was that the sunlight was interfering with the tachometer's ability to record the reflected light the sticker. Another issue is that the reflective sticker was placed on a small piece of white PVC pipe. The sunlight could have potentially been reflected off the PVC in addition to the sticker, leading to inaccurate values. While we did try to block the sunlight by hand and orient the tachometer in positions that reduced sunlight exposure, many of the values we recorded were still inaccurate.

5. Conclusion

The turbine developed in this project is a proof of concept. With the proper charging circuit, the turbine could be adapted to charge small electronic devices such as battery packs or cell phones. While we were successful in designing and building a turbine that required little machining, it did not meet the electrical output we desired. We had expected the turbine to produce 8W of power but the maximum power achieved during testing was 4W. Future improvements can be made to not only improve the performance of the turbine but also the accuracy of the data recorded.

We used a laser tachometer to measure the RPM of the turbine, but at times the tachometer could not accurately record RPMs because of the reflection from the sun. Using a contact tachometer to measure the RPMs would remove any variations in the measurements caused by the sun, giving us more accurate readings. Additionally, we used a simple unidirectional anemometer to measure the wind speed, but the area we tested the turbine had intermittent, swirling wind, making it was difficult to measure the wind speed. To improve the wind speed measurement accuracy, we would place the turbine in an open area to reduce and record the wind speed with an omnidirectional anemometer. Additionally, we could record all voltage, RPM, and wind speed data electronically using a data logger. This would give us precise instantaneous measurements, which would allow us to calculate any lag between the RPM and wind speed values caused by vortices or fluctuation in wind speed. By having the wind speed data electronically saved, it would be possible to average the wind speed to accurately match the wind speed with the RPM of the turbine.

Another improvement we would make is modifying the tower structure to reduce vibrations. The current tower design incorporates many reducers which makes the connection between the legs and main shaft weak. According to theoretical calculations the main shaft should only have deflected 27.95 mm. However, video analysis shows that the turbine actually deflects 49.3 mm in 15 m/s wind speeds. This excess deflection reduced the turbine's efficiency since a portion of the available wind energy is being lost to vibration. Improving the design can be done by redesigning the tower so that the main shaft is supported at two points instead of just one.

Another method to increase the power output is to improve the power matching of the turbine and the generator. When we first matched the turbine and the generator, we did not take into account any vibrational and frictional losses. These losses resulted in a decrease in power produced by the turbine. This made the gearing ratio we selected not ideal because it prevented the turbine from operating most efficiently. By changing the gearing ratio or choosing a different motor that better matches our turbine's power, we can improve the power output of the turbine system.

The final method of improving the wind turbine performance is decreasing the turbine solidity by shortening the chord length of the blades. This would allow more wind to flow through the swept area of the turbine, which allows the blades to extract more energy from the wind. In general, as the solidity decreases, the peak power coefficient of a wind turbine increases and is shifted to a higher tip speed ratio. However, decreasing the solidity too much could also lower the turbine efficiency as well. Our turbine has a very high solidity of 1.08, which was intended to aid in self-starting by producing more torque in low wind conditions. However, since the efficiency of the turbine was lower than expected and it still had difficulty self-starting, it

would be reasonable decrease the solidity. This would have the additional benefit of decreasing the blade mass and rotor inertia, allowing the turbine respond faster to changing wind speeds and possibly decreasing start-up time. Finally, the increased optimal tip speed ratio means that the turbine would operate at a higher rotational speed. Consequently, the generator would rotate faster allowing it to produce higher voltages for given wind speeds. This in turn would increase the generator efficiency by reducing internal resistive losses, resulting in a higher system efficiency.

References

[1] R. Meyer, "What's Happening With the Relief Effort in Puerto Rico?" The Atlantic, 2017. Available: https://www.theatlantic.com/science/archive/2017/10/what-happened-in-puerto-rico-a-timeline-of-hurricane-maria/541956/.

[2] P. Mazzei and F. Robles, "Parts of Puerto Rico Won't Have Power for 8 Months. What's the Holdup?" New York Times, 2017. Available: https://www.nytimes.com/2017/12/23/us/puerto-rico-power-outage.html.

[3] R. Pérez-Peña, "After Irma and Maria: How 3 Spots on the U.S. Virgin Islands Are Faring," New York Times, 2017. Available: https://www.nytimes.com/2017/11/10/us/virgin-islands-hurricanes.html.

[4] T. Craig, "Hurricanes left behind mountains of trash in the Virgin Islands — and there's nowhere to put it," The Washington Post, 2018. Available: https://www.washingtonpost.com/national/mountains-of-trash-left-behind-by-hurricanes-inflame-debate-in-us-virgin-islands/2018/02/22/30763f0e-1008-11e8-9065-e55346f6de81_story.html?noredirect=on&utm_term=.638124ddfe54.

[5] (Random House Dictionary). Renewable Energy. Available: http://www.dictionary.com/browse/renewable-energy.

[6] P. Dykstra, "History of environmental movement full of twists, turns " 2008. Available: http://www.cnn.com/2008/TECH/science/12/10/history.environmental.movement/index.html.

[7] Z. Shahan. (November 21,). History of Wind Turbines. Available: http://www.renewableenergyworld.com/ugc/articles/2014/11/history-of-wind-turbines.html.

[8] (United States Energy Information Administration). What is U.S. electricity generation by energy source?. Available: https://www.eia.gov/tools/faqs/faq.php?id=427&t=3.

[9] (United States Department of Energy). Energy Incentive Programs. Available: https://energy.gov/eere/femp/energy-incentive-programs.

[10] T. Burton et al, Wind Energy Handbook. (2nd ed.) West Sussex, United Kingdom: John Wiley & Sons, Ltd, 2011.

[11] G. L. Johnson, Wind Energy Systems. Englewood Cliffs, N.J: Prentice-Hall, 1985.

[12] M. Ragheb, Vertical Axis Wind Turbine. 2015.

[13] J. L. Tangler and D. M. Somers. J. L. Tangler and D. M. Somers. NREL airfoil families for HAWTs. NREL airfoil families for HAWTs. USDOE, Washington, DC (United States). USDOE, Washington, DC (United States). United States. United States. 1995Available: http://www.osti.gov/scitech/biblio/10106095. DOI: 10.2172/10106095.

[14] Mohammad Sadraey and Daniel Webster College, "Chapter 5 Wing Design," 2013.

[15] M. Nakamura. Airfoil. Available: http://web.mit.edu/2.972/www/reports/airfoil/airfoil.html.

[16] K. Zipp. (January 18,). Gears & Gearboxes 101. Available: http://www.windpowerengineering.com/design/mechanical/gearboxes/gears-gearboxes-101/.

[17] Turbinesinfo, "Horizontal Axis Wind Turbines – HAWT - Turbines Info," 2011. Available: http://www.turbinesinfo.com/horizontal-axis-wind-turbines-hawt/.

[18] W. Tjiu et al, "Darrieus vertical axis wind turbine for power generation I: Assessment of Darrieus VAWT configurations," Renewable Energy, vol. 75, pp. 50-67, 2015. Available: http://www.sciencedirect.com/science/article/pii/S096014811400603X. DOI: 10.1016/j.renene.2014.09.038.

[19] A. Alaimo et al, "Analysis of different blade architectures on small VAWT Performance," Energies, vol. 8, (4), pp. 3013-3033, 2015. Available: https://search.proquest.com/docview/1676103309. DOI: 10.3390/en8043013.

[20] P. Gipe, Wind Power. (Rev. and expanded ed. ed.) White River Junction, Vt: Chelsea Green Publ. Co, 2004.

[21] J. V. Akwa, H. A. Vielmo and A. P. Petry, "A review on the performance of Savonius wind turbines," Renewable and Sustainable Energy Reviews, vol. 16, (5), pp. 3054-3064, 2012. Available: http://www.sciencedirect.com/science/article/pii/S1364032112001505. DOI: 10.1016/j.rser.2012.02.056.

[22] J. P. Abraham et al, "Summary of Savonius wind turbine development and future applications for small-scale power generation," Journal of Renewable and Sustainable Energy, vol. 4, (4), pp. 42703, August, 2012.

[23] E. Hau, Wind Turbines : Fundamentals, Technologies, Application, Economics.

[24] M. R. Patel, Wind and Solar Power Systems. (2. ed. ed.) 2006.

[25] R. Fitzpatrick. The Direct Current Generator. Available: http://farside.ph.utexas.edu/teaching/302l/lectures/node91.html.

[26] Crouzet, "Some Principals of Direct Current (DC) Motors," .

[27] (Pololu). Motor Curve. Available: https://www.pololu.com/picture/view/0J6476.

[28] A. Bianchini, G. Ferrara and L. Ferrari, "Design guidelines for H-Darrieus wind turbines: Optimization of the annual energy yield," Energy Conversion & Management, vol. 89, pp. 690-707, 2015. Available: https://www.sciencedirect.com/science/article/pii/S0196890414009194. DOI: 10.1016/j.enconman.2014.10.038.

[29] J. H. Strickland. The darrieus turbine: A performance prediction model using multiple streamtubes. Sandia National Laboratories. Sandia National Laboratories. 1975Available: http://prod.sandia.gov/techlib/access-control.cgi/1975/750431.pdf.

[30] D. Vallverdu, D. Rempfer and P. Kozak, "VAWT Analysis," vol. 1.16, Nov 10, 2015.

[31] R. E. Sheldahl and P. C. Klimas, "Aerodynamic characteristics of seven symmetrical airfoil sections through 180-degree angle of attack for use in aerodynamic analysis of vertical axis wind turbines," Sandia National Laboratories, Mar. 1981.

Appendices

Appendix A: Plots of power output versus wind speed for different turbine heights

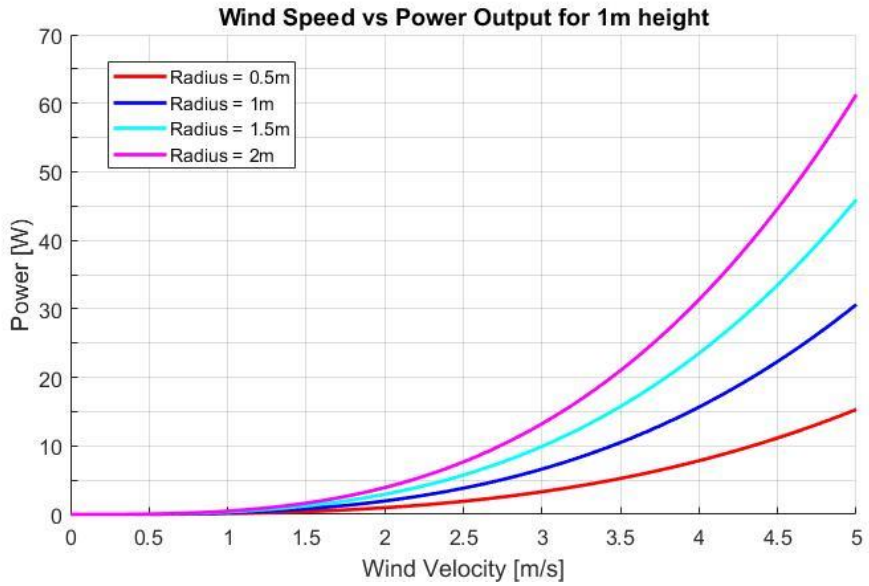

Figure 26: Plot of power vs wind velocity for 1 meter tall VAWT with varying blade sizes

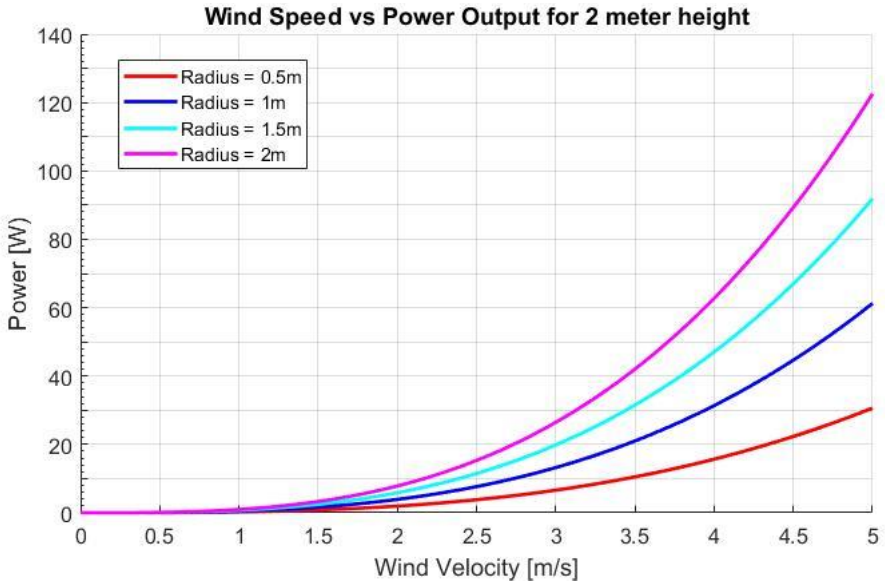

Figure 27: Plot of torque vs wind velocity for 2 meter tall VAWT with varying blade sizes

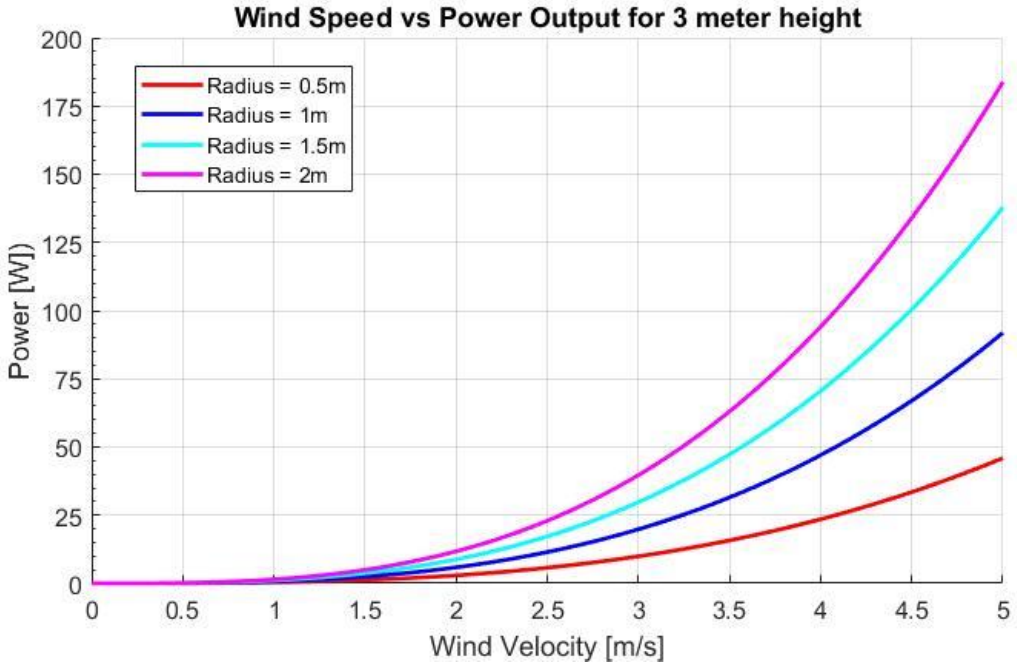

Figure 28: Plot of torque vs wind velocity for 3 meter tall VAWT with varying blade sizes

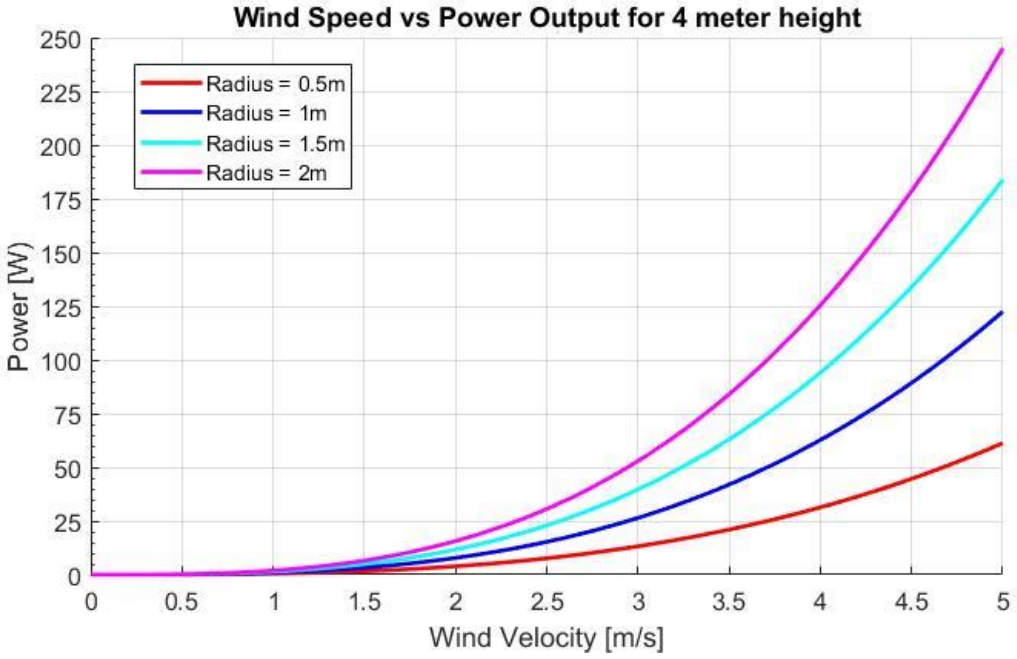

Figure 29: Plot of torque vs wind velocity for 4 meter tall VAWT with varying blade sizes

Appendix B: Plots of torque versus wind speed for different turbine heights

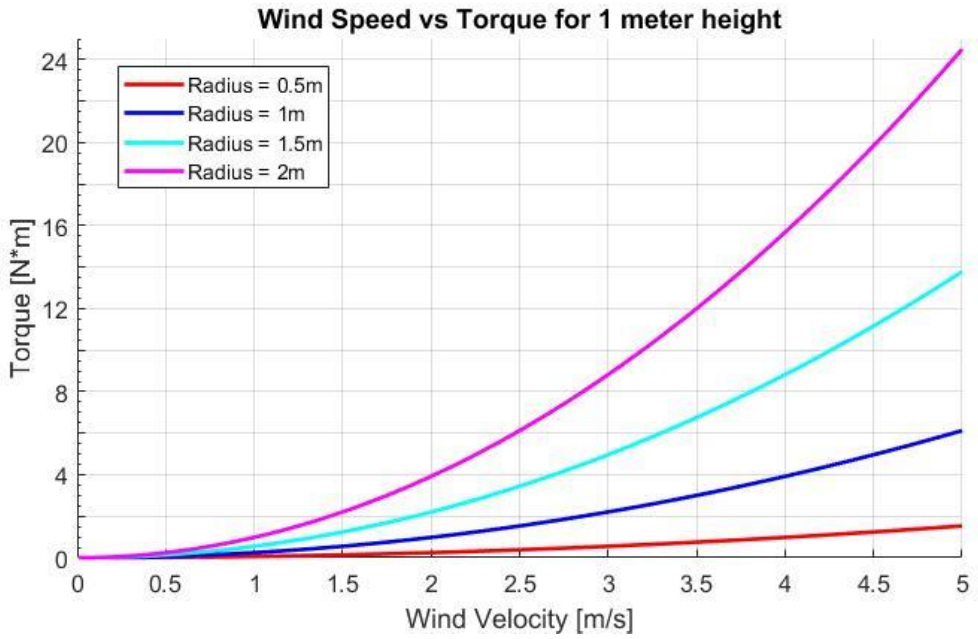

Figure 30: Plot of torque vs wind velocity for 1 meter tall VAWT with varying blade sizes

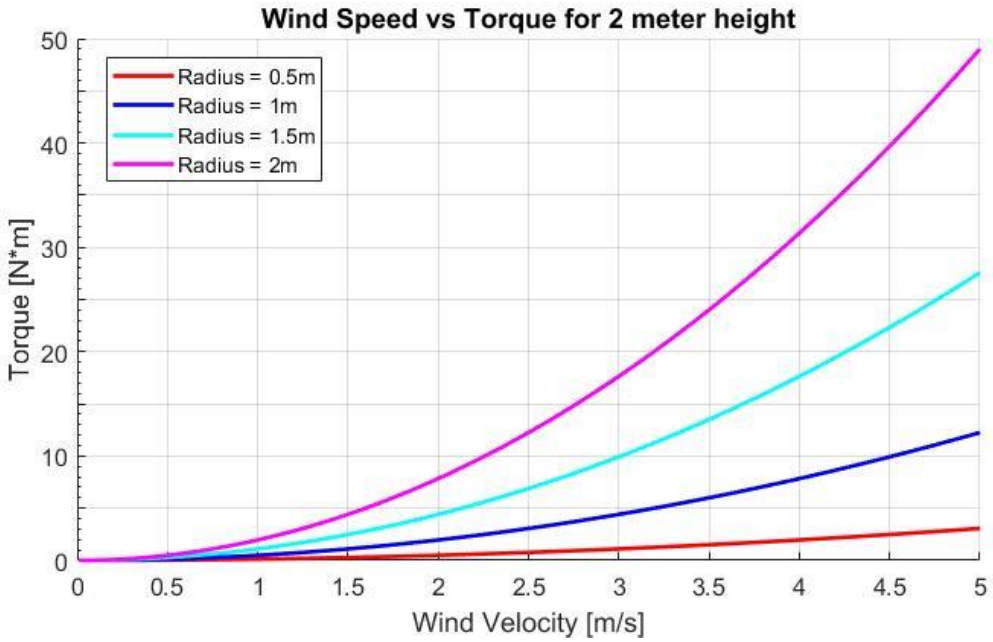

Figure 31: Plot of torque vs wind velocity for 2 meter tall VAWT with varying blade sizes

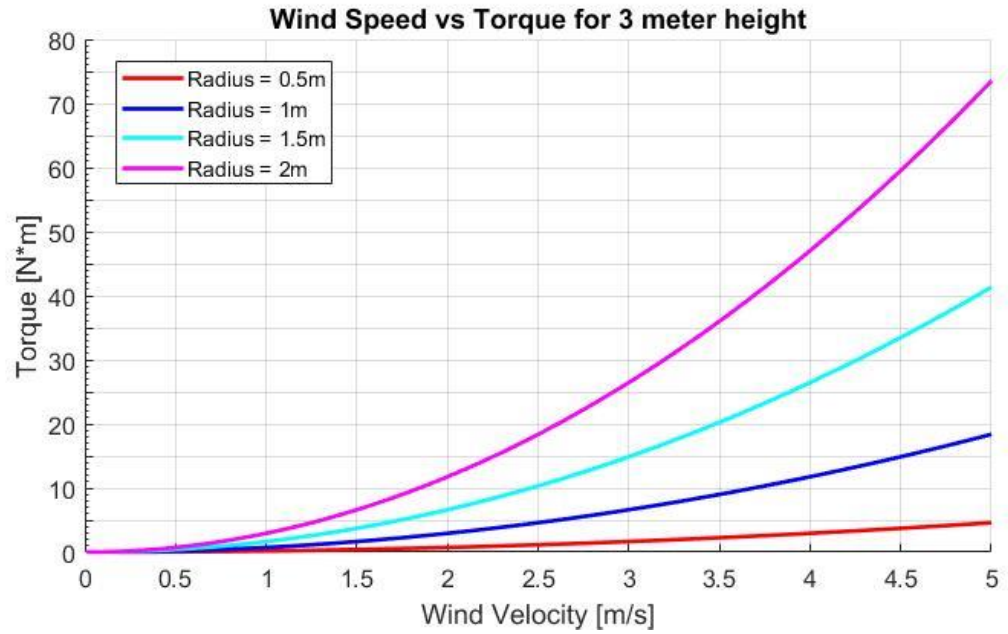

Figure 32: Plot of torque vs wind velocity for 3 meter tall VAWT with varying blade sizes

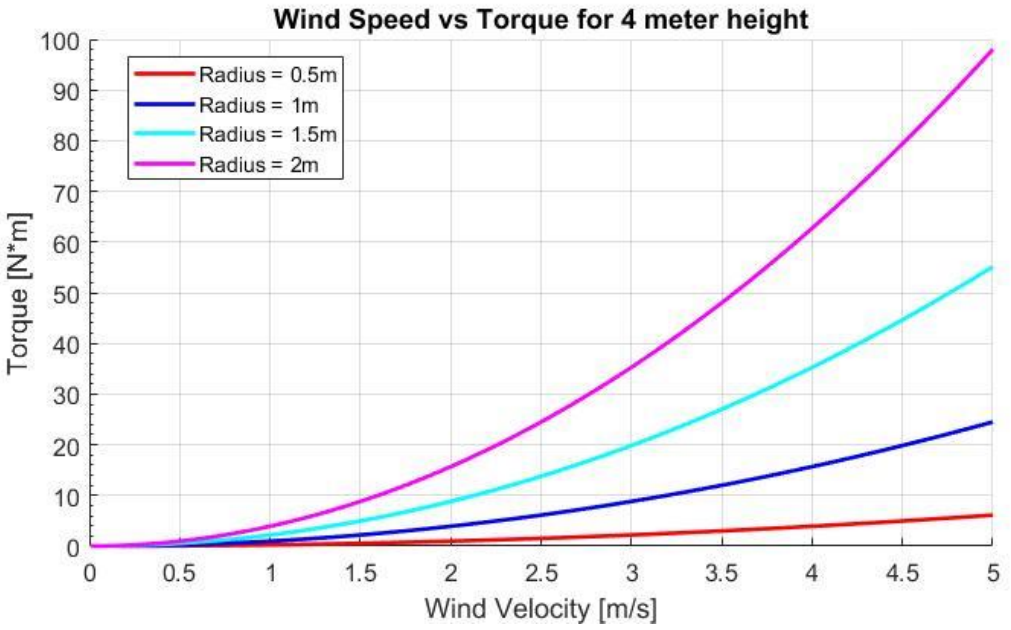

Figure 33: Plot of torque vs wind velocity for 4 meter tall VAWT with varying blade sizes

Appendix C: Calculation of main shaft deflection without motor mount legs

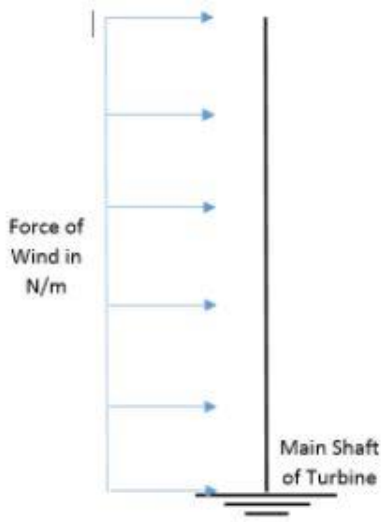

Figure 34: Force diagram for main shaft without motor mount legs in steady wind

Initial Variables

Shaft Length: $L := 5ft = 1.524\,m$

Shaft Modulus of Elasticity: $E := 200 \cdot 10^{3} MPa$

Moment of Inertia for shaft: $I := 14151 mm^{4}$

Force of wind at 5 m/s: $Fthrust := \frac{34.97N}{L} = 22.946 \cdot \frac{N}{m}$

Reaction Forces

$M_1 := Fthrust \cdot L \cdot \frac{L}{2} = 26.647 \cdot N \cdot m$ $\quad$ $Rx := Fthrust \cdot L = 34.97 \cdot N$

Singularity Functions

Initial Conditions

$S(x,z) := if(x \geq z, 1, 0)$ $\quad$ $n(x,z) := if(x \neq z, 0, \infty)$ $\quad$ $x := 0, 0.001 \cdot L .. L$

Force Equation

$$Q(x) := Rx \cdot n(x,0)\,(x-0)^{-1} - Fthrust \cdot S(x,0) \cdot (x-L)^{0}$$

Shear Equation

$$v(x) := Rx \cdot S(x,0)\,(x-0)^{0} - Fthrust \cdot S(x,0) \cdot (x-L)^{1}$$

Moment Equation

$$M(x) := Rx \cdot S(x,0)\,(x-0)^1 - \frac{Fthrust}{2} \cdot S(x,0) \cdot (x-L)^2$$

Angle Equation

$$\theta(x) := \frac{1}{E \cdot I} \cdot \left[\frac{Rx}{2} \cdot S(x,0)\,(x-0)^2 - \frac{Fthrust}{6} \cdot S(x,0) \cdot (x-L)^3 \right]$$

Deflection Equation

$$\delta(x) := \frac{1}{E \cdot I} \cdot \left[\frac{Rx}{6} \cdot S(x,0)\,(x-0)^3 - \frac{Fthrust}{24} \cdot S(x,0) \cdot (x-L)^4 \right]$$

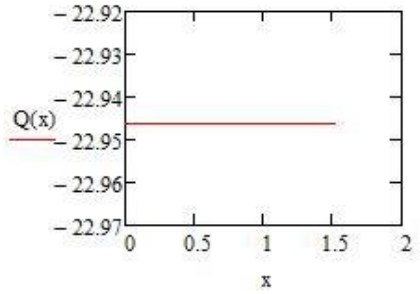

Figure 37: Plot of force as a function of distance from main shaft

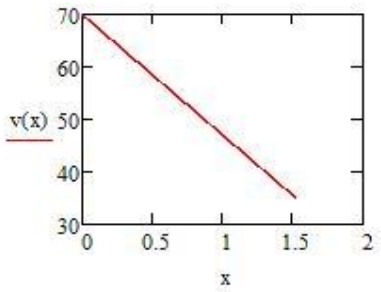

Guess

$t := 1.5m$

Given

$Q(t) := 0$

$sol := root(Q(t), t) = 1.5\,m$

$V_{max} := |v(sol)| = 35.521\,N$

Figure 35: Plot of shear force as a function of distance from main shaft

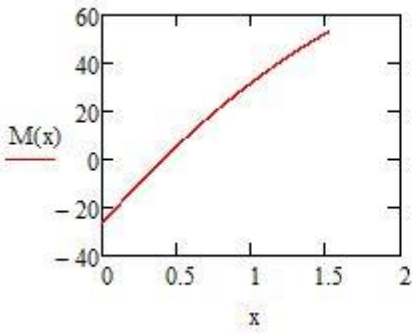

Guess

$u := 1.5m$

Given

$V(u) := 0$

$x_{calc} := root(V(u), u) = 1.5\,m$

$M_{max} := \left|M\left(x_{calc}\right)\right| = 52.448\,m \cdot N$

Figure 36: Plot of moment as a function of distance from main shaft

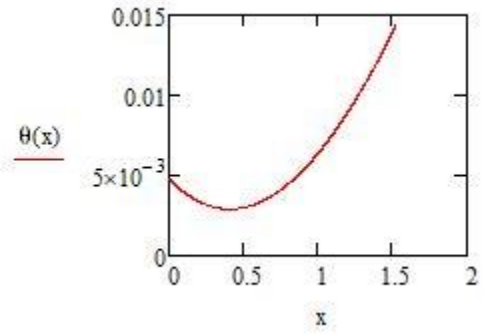

Figure 39: Plot of deflection angle as a function of distance from main shaft

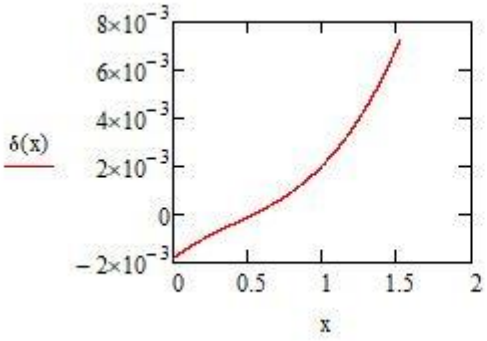

Guess

$p := 1.5m$

Given

$\theta(p) := 0$

$x_{calc} := root(\theta(p), p) = 1.5\,m$

$\left|\delta(x_{calc})\right| = 6.95 \cdot mm$

Figure 38: Plot of deflection as a function of distance from main shaft

Appendix D: Calculation of main shaft deflection with motor mount legs

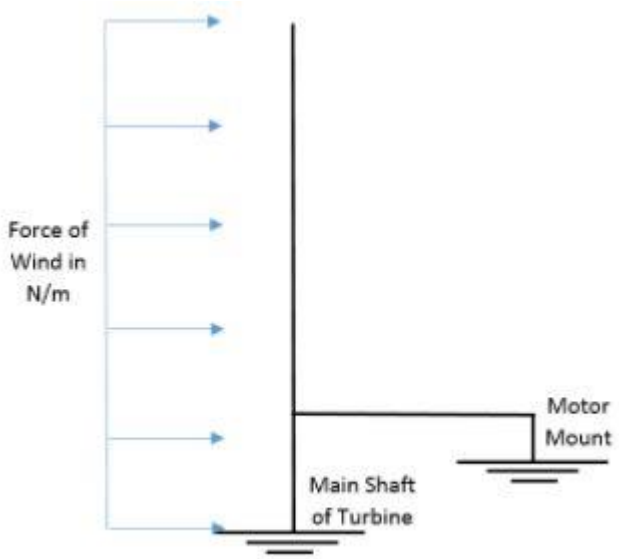

Figure 40: Force diagram for main shaft with motor mount legs in steady wind

Initial Variables

Shaft Length: $L := 5ft = 1.524\,m$

Shaft Modulus of Elasticity: $E := 200 \cdot 10^3 MPa$

Moment of Inertia for shaft: $I := 14151 mm^4$

Force of wind at 5 m/s: $Fthrust := \frac{314N}{L} = 206.037 \cdot \frac{N}{m}$

Distance from base of shaft to motor attachment bracket $B := 3in$

Reaction Forces

$$R_2 := \frac{Fthrust \cdot L \cdot \frac{L}{2}}{B} = 3.14 \times 10^3 N$$

$$R_1 := Fthrust \cdot L - R_2 = -2.826 \times 10^3 N$$

Singularity Functions

Initial Conditions

$S(x,z) := if(x \geq z, 1, 0)$ $n(x,z) := if(x \neq z, 0, \infty)$ $x := 0, 0.001 \cdot L .. L$

Force Equation

$$Q(x) := R_1 \cdot n(x,0)\,(x-0)^{-1} + R_2 \cdot n(x,B) \cdot (x-B)^{-1} - Fthrust \cdot S(x,0) \cdot (x-L)^{0}$$

Shear Equation

$$v(x) := R_1 \cdot S(x,0)\,(x-0)^{0} + R_2 \cdot S(x,B) \cdot (x-B)^{0} - Fthrust \cdot S(x,0) \cdot (x-L)^{1}$$

Moment Equation

$$M(x) := R_1 \cdot S(x,0)\,(x-0)^{1} + R_2 \cdot S(x,B) \cdot (x-B)^{1} - \frac{Fthrust}{2} \cdot S(x,0) \cdot (x-L)^{2}$$

Angle Equation

$$\theta(x) := \frac{1}{E \cdot I} \cdot \left[\frac{R_1}{2} \cdot S(x,0)\,(x-0)^{2} + \frac{R_2}{2} \cdot S(x,B) \cdot (x-B)^{2} - \frac{Fthrust}{6} \cdot S(x,0) \cdot (x-L)^{3} \right]$$

Deflection Equation

$$\delta(x) := \frac{1}{E \cdot I} \cdot \left[\frac{R_1}{6} \cdot S(x,0)\,(x-0)^{3} + \frac{R_2}{6} \cdot S(x,B) \cdot (x-B)^{3} - \frac{Fthrust}{24} \cdot S(x,0) \cdot (x-L)^{4} \right]$$

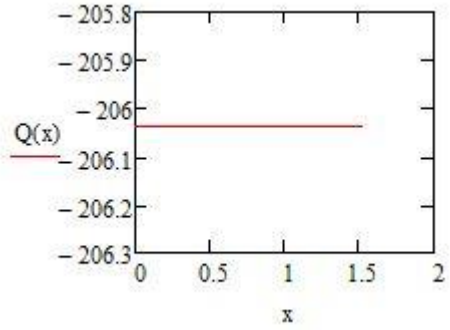

Figure 42: Plot of force as a function of distance

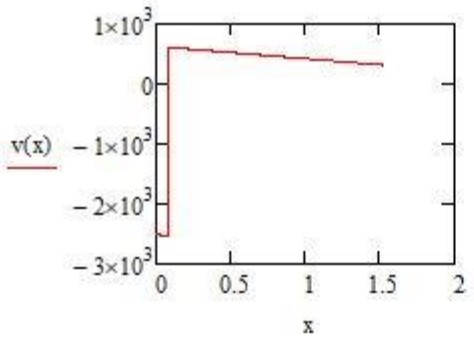

Guess

guess := 1.5m

Given

Q(guess) := 0

sol := root(Q(guess), guess) = 1.5 m

$V_{max} := |v(guess)| = 318.945\,N$

Figure 41: Plot of shear force as a function of distance

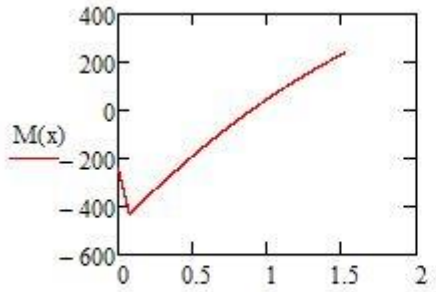

Guess

$u := 1.5m$

Given

$V(u) := 0$

$x_{calc} := root(V(u), u) = 1.5\,m$

$M_{max} := |M(x_{calc})| = 231.673\,m \cdot N$

Figure 43: Plot of moment as function of distance

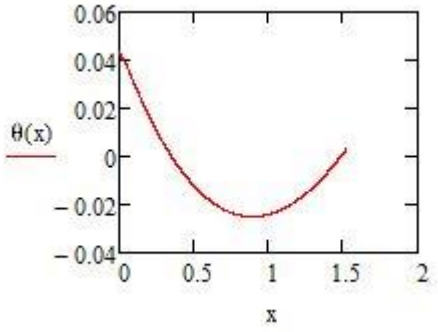

Figure 45: Plot of deflection angle as function of distance

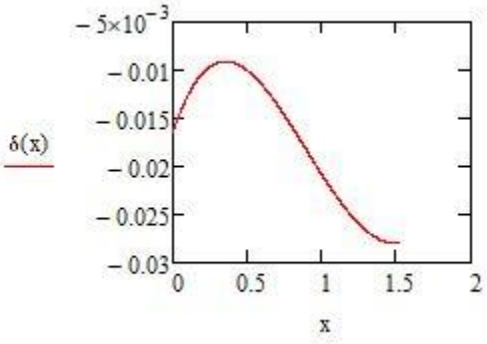

Guess

$p := 1.5m$

Given

$\theta(p) := 0$

$x_{calc} := root(\theta(p), p) = 1.5\,m$

$|\delta(x_{calc})| = 27.952 \cdot mm$

Figure 44: Plot of deflection as function of distance

Appendix E: Calculation of outer shaft deflection

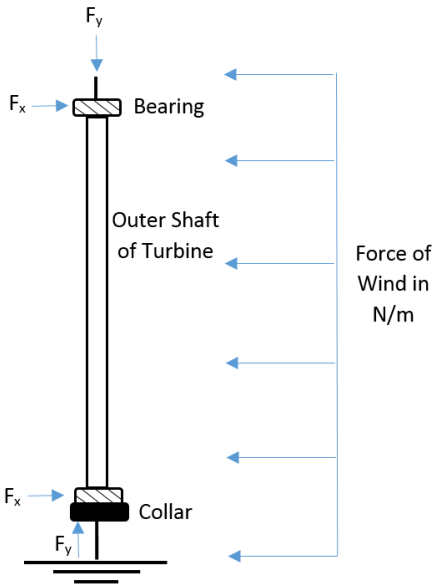

Figure 46: Force diagram for turbine outer shaft in steady wind

Initial Variables

Shaft Length: $L := 33in = 0.838m$

Shaft Modulus of Elasticity: $E := 2830 \cdot 10^3 MPa$

Moment of Inertia for shaft: $I := 27887.51mm^4$

Force of wind at 5 m/s: $Fthrust := \frac{34.97N}{L} = 41.72 \cdot \frac{N}{m}$

Reaction Forces

$$R_2 := \frac{Fthrust \cdot L \cdot \frac{L}{2}}{L} = 17.485N$$

$$R_1 := Fthrust \cdot L - R_2 = 17.485N$$

Singularity Functions

Initial Conditions

$S(x,z) := if(x \geq z, 1, 0)$ $n(x,z) := if(x \neq z, 0, \infty)$ $x := 0, 0.001 \cdot L .. L$

Force Equation

$$Q(x) := R_1 \cdot n(x,0)\,(x-0)^{-1} + R_2 \cdot n(x,L) \cdot (x-L)^{-1} - Fthrust \cdot S(x,0) \cdot (x-L)^{0}$$

Shear Equation

$$v(x) := R_1 \cdot S(x,0)\,(x-0)^{0} + R_2 \cdot S(x,L) \cdot (x-L)^{0} - Fthrust \cdot S(x,0) \cdot (x-L)^{1}$$

Moment Equation

$$M(x) := R_1 \cdot S(x,0)\,(x-0)^{1} + R_2 \cdot S(x,L) \cdot (x-L)^{1} - \frac{Fthrust}{2} \cdot S(x,0) \cdot (x-L)^{2}$$

Angle Equation

$$\theta(x) := \frac{1}{E \cdot I} \cdot \left[\frac{R_1}{2} \cdot S(x,0)\,(x-0)^{2} + \frac{R_2}{2} \cdot S(x,L) \cdot (x-L)^{2} - \frac{Fthrust}{6} \cdot S(x,0) \cdot (x-L)^{3} \right]$$

Deflection Equation

$$\delta(x) := \frac{1}{E \cdot I} \cdot \left[\frac{R_1}{6} \cdot S(x,0)\,(x-0)^{3} + \frac{R_2}{6} \cdot S(x,L) \cdot (x-L)^{3} - \frac{Fthrust}{24} \cdot S(x,0) \cdot (x-L)^{4} \right]$$

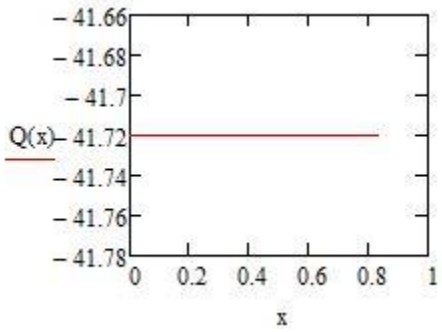

Figure 48: Plot of wind force on outer shaft as a function of distance

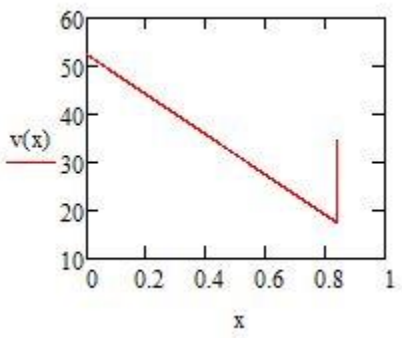

Guess

$f := 0.419\,m$

Given

$Q(f) := 0$

$sol := root(Q(f), f) = 0.419\,m$

$V_{max} := |v(sol)| = 34.974\,N$

Figure 47: Plot of shear force on outer shaft as a function of distance

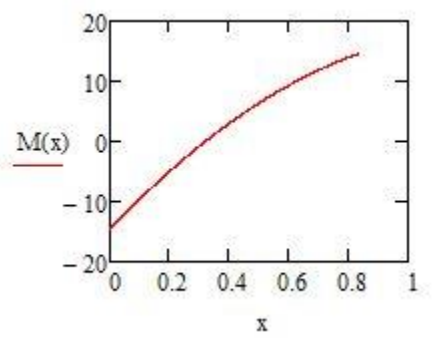

Guess
$u := 0.419m$
Given
$V(u) := 0$
$x_{calc} := root(V(u), u) = 0.419\,m$
$M_{max} := |M(x_{calc})| = 3.66\,m \cdot N$

Figure 51: Plot of moment on outer shaft as a function of distance

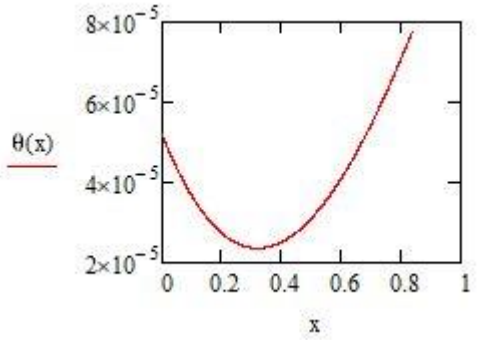

Figure 51: Plot of outer shaft deflection angle as a function of distance

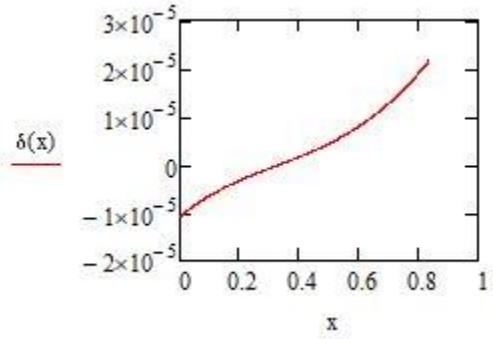

Guess
$p := 0.419m$
Given
$\theta(p) := 0$
$x_{calc} := root(\theta(p), p) = 0.419\,m$
$|\delta(x_{calc})| = 2.036 \times 10^{-3}\,mm$

Figure 51: Plot of main shaft deflection as a function of distance